

CiTrus: Squeezing Extra Performance out of Low-data Bio-signal Transfer Learning

Eloy Geenjaar^{1*}
Lie Lu²

¹Georgia Institute of Technology
²Dolby Laboratories
egeenjaar@gatech.edu, llul@dolby.com

Abstract

Transfer learning for bio-signals has recently become an important technique to improve prediction performance on downstream tasks with small bio-signal datasets. Recent works have shown that pre-training a neural network model on a large dataset (e.g. EEG) with a self-supervised task, replacing the self-supervised head with a linear classification head, and fine-tuning the model on different downstream bio-signal datasets (e.g., EMG or ECG) can dramatically improve the performance on those datasets. In this paper, we propose a new convolution-transformer hybrid model architecture with masked auto-encoding for low-data bio-signal transfer learning, introduce a frequency-based masked auto-encoding task, employ a more comprehensive evaluation framework, and evaluate how much and when (multimodal) pre-training improves fine-tuning performance. We also introduce a dramatically more performant method of aligning a downstream dataset with a different temporal length and sampling rate to the original pre-training dataset. Our findings indicate that the convolution-only part of our hybrid model can achieve state-of-the-art performance on some low-data downstream tasks. The performance is often improved even further with our full model. In the case of transformer-based models we find that pre-training especially improves performance on downstream datasets, multimodal pre-training often increases those gains further, and our frequency-based pre-training performs the best on average for the lowest and highest data regimes.

Introduction

The wearable market is growing quickly around the world (Casselman, Onopa, and Khansa 2017). This increase in wearable usage means there is an increasing amount of bio-signal data available that can be used in the field of preventative medicine. Bio-signals can also complement a doctor’s qualitative data. By combining subjective assessments of experiences with objective signals extracted from bio-signals related to someone’s well-being, stress level, cognitive state, etc., doctors can make more informed treatment decisions. There are many types of bio-signals, each recording a different type of information, for example, electroencephalography (EEG) non-invasively records

the brain’s electrical activity from outside the skull and can be used to predict attention levels (Li et al. 2011). On the other hand, photoplethysmography (PPG) records volumetric blood changes, and can be used to predict stress levels (Charlton et al. 2018) from non-invasive recordings on the skin. Many more bio-signals exist, each with unique information about a potential patient.

However, bio-signals also come with three important drawbacks. First, bio-signals are noisy; with EEG, for example, the electrical activity from the brain is recorded through the skull and thus must travel through a dense bone before it arrives at the electrodes, which leads to noise. Moreover, it is harder to record activity deeper in the brain because the further away electrical current is generated from the electrode, the harder it is to reliably capture it. In addition to fundamental limitations of non-invasive bio-signals, especially for wearables, normal activities like movement can induce a lot of noise in the signal. Secondly, bio-signals suffer from a lot of subject-variability, i.e., it can be hard to generalize predictions from one person’s bio-signal to the same bio-signal recorded from another person. Lastly, making predictions about a person’s internal state from bio-signals is often non-trivial. These predictions require complex and non-linear transformations of the original bio-signal. This has led to the wide-scale adoption of neural networks in bio-signal research. However, neural networks require substantial amounts of labeled data to train on, and labeling bio-signals is expensive because it requires (medical) experts to go through the data and label individual time windows of each bio-signal. It is thus imperative to develop neural network models that do not require many examples to train on.

Transfer learning mitigates the need for many examples by first pre-training a neural network on a larger dataset. Transfer learning has shown to be effective for bio-signals with models pre-trained using a self-supervised task (Zhang et al. 2022; Liu et al. 2023; Dong et al. 2024). In this work, we develop a comprehensive evaluation strategy for bio-signal transfer learning and find that convolution-based architectures often outperform transformer-only models. In doing so, we propose a new convolution transformer hybrid model that we call CiTrus and a new pre-training and fine-tuning strategy. Our model systematically improves performance over previous methods and strong baselines we introduce for comparison in this paper.

*Work was done during an internship at Dolby Laboratories
Copyright © 2025, Association for the Advancement of Artificial Intelligence (www.aaai.org). All rights reserved.

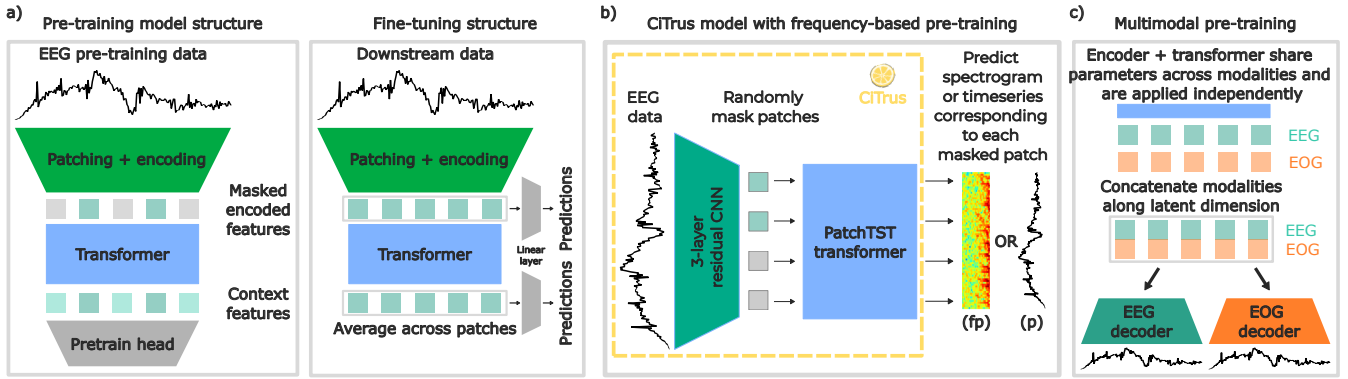


Figure 1: Subfigure a) shows the general transfer learning framework; the pre-training and fine-tuning structures. Subfigure b) shows the pre-training structure of our proposed model, and sub-figure c) shows how the structure of the model is adapted to accommodate multi-modal pre-training data.

In summary, our main contributions are:

- The introduction of a convolution and transformer hybrid for bio-signals (CiTrus) that outperforms all previous models by a significant margin.
- A spectrogram-based pre-training approach that forces the model to learn the relationship between the bio-signal time-series and its frequency spectrum, improving fine-tuning performance.
- A new transferring approach that keeps the sampling frequency the same between the pre-training and fine-tuning dataset, which for most datasets, significantly improves performance.
- A more comprehensive evaluation of transfer learning models for bio-signals. We add new datasets, evaluate the models over multiple data availability regimes, and use multiple test splits. We find that each of these is important for a fair comparison of bio-signal transfer learning.

Background

Transfer learning The goal of transfer learning is to develop a model that transfers well to downstream datasets with few labeled examples after pre-training. Specifically with bio-signals, these downstream datasets are time series data, often with a unique temporal length, sampling frequency, and a variety of different prediction targets. Labels in the datasets are provided for windows over time, e.g. when is a cardiac rhythm normal and when is it indicative of atrial fibrillation. A common self-supervised method for pre-training is masked auto-encoding (He et al. 2022), which has also been used for bio-signal transfer learning previously (Liu et al. 2023; Dong et al. 2024). Specifically, masked autoencoding models can be loosely split into two parts; a patching and encoding part (encoder), and a transformer, see Figure 1a. In the simplest case, the patching and encoding part of the model linearly embeds non-overlapping segments (patches) of the input signal into latents, see Figure 1a. We refer to these latents as encoded features. The encoded features are then randomly masked by replacing the

patches with a mask token, and used as input to the transformer, which produces context features. These are in turn used to predict the original signal that corresponds to the masked patches with the pretrain head that can be any type of neural network architecture, for example a linear layer or a multi-layer perceptron. The transformer learns temporal relationships between patches that allow it to predict the masked patches.

After pre-training the model, the pretrain head is removed from the model, and in the fine-tuning stage, a linear layer is attached either to the encoded features (after the encoder) or the context features (after the transformer), see Figure 1a. The linear layer, together with the rest of the model, is trained on the downstream bio-signal dataset. The assumption behind this method is that the relevant features and patch relationships the transformer and/or the encoder have learned are transferable to new bio-signal datasets and are a good starting point for supervised training.

Related work In the supervised and decoding literature for EEG data, convolution-transformer hybrids have shown improvements over convolution-only architectures on a variety of tasks (Song et al. 2022; Peh, Yao, and Dauwels 2022; Gong et al. 2023; Miltiadous et al. 2023). However, all of these methods are specifically developed for EEG, are fully supervised, and have spatial convolution blocks that make it hard for them to transfer to new data with a different number of channels. Moreover, the field of masked auto-encoding for EEG and bio-signal data has recently seen many advances in same-data pre-training and fine-tuning (Chien et al. 2022; Yang, Westover, and Sun 2024), representation learning (Foumani et al. 2024), semi-supervised learning (Eldele et al. 2023), and cross-modal learning (Deldari et al. 2023). These models do not perform pre-training on one bio-signal with fine-tuning on a new bio-signal, however.

One reason why transfer learning from one bio-signal dataset to another dataset likely works is because the important frequency ranges are similar across bio-signals and transfer learning makes it easier to find features similar to the ones found during pre-training (Neyshabur, Sedghi, and

Dataset	EMG@20%			ECG@0.5%			PPG@10%			HAR@10%		
Metric	ACC	ROC	PRC	ACC	ROC	PRC	ACC	ROC	PRC	ACC	ROC	PRC
PatchTST (s)	51.46	61.87	52.07	54.15	52.34	60.85	59.98	73.89	55.32	67.67	88.62	69.83
PatchTST (p)	57.93	71.35	62.46	56.63	52.89	61.34	59.74	74.57	56.31	60.57	85.85	62.7
bioFAME (s)	50.43	61.89	53.46	58.36	51.66	60.52	60.31	73.98	55.2	54.03	84.31	56.72
bioFAME (mp)	70.93	86.94	78.78	64.26	52.89	61.36	60.21	<u>76.67</u>	58.51	60.5	86.85	65.54
NLPatchTST (s)	64.64	81.15	71.84	52.28	51.92	60.53	56.81	72.27	53.42	68.54	88.94	70.01
NLPatchTST (p)	70.45	87.9	80.11	54.43	52.96	61.27	60.39	75.15	56.62	65.66	87.78	67.61
NLPatchTST (mp)	74.61	90.16	82.77	56.86	53.02	61.41	59.44	74.78	56.14	60.41	86.2	63.7
SimMTM (s)	52.73	84.79	75.52	58.47	53.56	61.86	54.53	<u>76.83</u>	<u>59.49</u>	<u>75.41</u>	<u>91.14</u>	<u>78.35</u>
SimMTM (p)	42.52	61.3	54.13	56.77	53.08	61.5	50.58	<u>73.7</u>	<u>56.07</u>	<u>77.37</u>	<u>91.76</u>	<u>80.14</u>
Ci (s)	<u>96.55</u>	<u>99.1</u>	<u>97.99</u>	66.89	<u>55.33</u>	<u>63.64</u>	58.91	72.12	54.47	80.71	93.03	82.8
Ci (p)	<u>94.74</u>	<u>98.72</u>	<u>96.73</u>	65.62	54.76	63.07	58.57	73.85	55.77	70.7	90.18	74.46
CiTrus (s)	<u>95.84</u>	99.48	99.4	<u>69.35</u>	<u>55.51</u>	<u>63.78</u>	59.18	72.35	56.03	71.87	89.97	74.89
CiTrus (p)	90.45	96.96	94.18	<u>64.55</u>	54.6	<u>62.84</u>	<u>62.41</u>	75.37	<u>59.14</u>	73.89	90.9	75.9
CiTrus (fp)	97.92	<u>99.02</u>	<u>98.76</u>	82.44	55.9	64.3	65.25	79.45	63.65	65.3	87.55	68.75
CiTrus (mp)	92.9	99.01	<u>96.86</u>	<u>67.72</u>	55.2	63.6	<u>62.98</u>	76.15	58.64	72.78	90.47	75.32
Dataset	FDB@0.5%			Epilepsy@1%			Gesture@10%			SleepEDF@0.5%		
Metric	ACC	ROC	PRC	ACC	ROC	PRC	ACC	ROC	PRC	ACC	ROC	PRC
PatchTST (s)	52.99	54.35	38.04	92.79	92.8	96.54	43.21	81.04	49.29	64.06	65.54	33.83
PatchTST (p)	60.15	55.91	39.59	93.34	93.81	97.09	49.6	83.79	56.36	<u>71.05</u>	67.8	36.33
bioFAME (s)	52.07	53.63	37.13	92.46	96.17	98.72	30.36	74.46	39.54	<u>70.62</u>	68.04	37.45
bioFAME (mp)	56.71	56.64	39.74	92.77	96.93	99.01	36.38	79.27	46.28	70.51	68.1	37.91
NLPatchTST (s)	58.61	56.81	39.68	84.03	78.38	88.43	43.35	82.06	50.31	58.59	64.53	33.79
NLPatchTST (p)	63.64	57.28	40.24	92.64	92.41	96.15	48.13	<u>84.6</u>	56.8	74.08	68.16	36.74
NLPatchTST (mp)	65.01	58.2	41.03	92.77	92.33	96.23	<u>51.88</u>	84.2	<u>57.39</u>	66.98	66.8	34.94
SimMTM (s)	43.26	52.69	36.45	93.35	55.15	86.21	<u>53.26</u>	<u>84.7</u>	63.2			
SimMTM (p)	68.89	60.59	44.66	93.21	55.03	85.63	56.83	85.43	<u>63.0</u>			
Ci (s)	<u>74.26</u>	<u>65.26</u>	<u>50.37</u>	93.75	<u>97.74</u>	<u>99.31</u>	35.09	75.98	43.72	69.02	69.03	38.84
Ci (p)	<u>72.72</u>	<u>64.45</u>	<u>48.88</u>	<u>94.37</u>	97.93	99.36	40.31	81.15	49.04	70.48	<u>68.58</u>	<u>38.57</u>
CiTrus (s)	72.34	63.87	47.85	93.2	97.68	99.17	42.77	81.6	51.08	67.61	67.75	36.41
CiTrus (p)	<u>75.48</u>	63.52	47.69	<u>94.08</u>	95.29	97.92	40.71	80.73	50.63	<u>73.87</u>	<u>68.85</u>	<u>37.96</u>
CiTrus (fp)	79.78	66.63	52.35	93.41	95.83	98.26	51.34	82.28	55.81	<u>48.69</u>	<u>58.11</u>	27.52
CiTrus (mp)	73.55	63.63	47.77	94.53	94.67	97.34	47.99	83.24	55.99	69.26	67.16	35.84

Table 1: A comparison of the different model architectures. We use the same evaluation method for each model, for EMG and FD-B we interpolate the data for fine-tuning, and for the other datasets we use our sliding window approach. The letters in brackets refer to how the model is trained; (s) is trained from scratch, (p) means it is pre-trained, (mp) means it uses multi-modal pre-training, and (fp) means it uses frequency pre-training. ACC, ROC, and PRC refer to the accuracy, area under the receiver operating characteristic, and the area under the precision recall curve, respectively. The best result for each metric is shown in bold, the second best result is double-underlined, and the third best result is single-underlined.

Zhang 2020). Frequency and time-frequency features are important for the analysis or predictions from bio-signals such as EEG (Duronbhan et al. 2019), ECG (Okinaka et al. 2010), and EMG (Weiderpass et al. 2013). Thus, learning features either directly in the frequency space or features that are consistent across time and frequency space can be helpful for downstream predictions. Time-frequency consistency (TFC) (Zhang et al. 2022) presents a method to extract features from the time and frequency domains that are trained to be similar. To do this they use contrastive learning, and introduce new frequency-based augmentations. Alternatively, bioFAME (Liu et al. 2023), introduces a Fourier neural operator (FNO)-based encoder (Li et al. 2020; Guibas et al. 2021) to directly model features in frequency space. Additionally, they use a frequency-aware masked autoencoder for

multimodal pre-training, and introduce PatchTST (Nie et al. 2022) as a baseline. Recently, SimMTM (Dong et al. 2024) has improved on TFC with the same model architecture by relating masked auto-encoding to manifold learning. They introduce a new pre-training task where the model needs to reconstruct the original timeseries with a set of masked timeseries outside the manifold. These previous works motivated us to develop a convolutional-transformer hybrid model (CiTrus), a frequency-based pre-training technique, and a better way of transferring a model from one bio-signal dataset to another.

Method

CiTrus: Convolution transformer hybrid Given the potential importance of the frequency representation in bio-

Dataset	EMG			ECG			PPG			HAR		
Data percentage	20%	50%	80%	0.5%	1%	2%	10%	20%	50%	10%	20%	50%
PatchTST	+18.7	-12.4	-11.1	+2.8	+3.5	+1.9	+1.1	+1.5	+1.3	-7.7	-6.2	-2.5
bioFAME	+49.0	+27.7	+10.0	+5.0	+4.4	+5.2	+3.3	-0.6	+2.0	+10.5	+7.9	+15.3
NLPatchTST (p)	+12.5	+1.9	+0.1	+3.4	-0.1	-0.1	+6.4	+2.5	-0.9	-2.9	-3.7	-0.8
NLPatchTST (mp)	+16.7	+1.0	-1.4	+5.6	+1.5	+1.1	+5.2	+1.8	+0.3	-7.8	-7.4	-1.7
SimMTM	-16.1	-3.2	-0.2	+3.5	-7.5	-3.5	-4.0	+0.2	-1.6	+2.0	+0.6	+0.5
Ci	-1.1	-0.3	-0.2	-0.8	-1.4	+1.9	+1.9	-0.2	+0.3	-8.5	-3.8	-0.3
CiTrus (p)	-4.4	-0.7	-0.2	-3.5	-1.2	+0.1	+6.5	+2.6	-0.3	+2.0	+2.3	-0.6
CiTrus (fp)	+0.4	-0.9	+0.3	+8.3	+8.9	+7.2	+12.9	+12.7	+9.0	-6.5	-4.2	-0.3
CiTrus (mp)	-2.0	-2.0	-0.2	-0.8	+0.5	+1.8	+7.1	+3.3	-1.4	+1.0	+2.4	-1.3
Dataset	FDB			Epilepsy			Gesture			SleepEDF		
Data percentage	0.5%	1%	2%	1%	5%	10%	10%	20%	50%	0.5%	1%	2%
PatchTST	+7.0	+6.9	-1.8	+0.8	-0.1	+0.0	+12.2	+8.7	+4.8	+7.3	+0.3	+1.3
bioFAME	+7.3	+8.9	+8.4	+0.5	+0.0	+0.1	+16.8	+11.8	+10.0	+0.4	+0.6	-1.2
NLPatchTST (p)	+4.1	+1.7	-3.1	+13.4	+15.0	+4.5	+11.4	+7.3	+4.4	+13.7	+4.4	+7.1
NLPatchTST (mp)	+6.1	+3.6	-1.1	+13.4	+15.6	+4.4	+15.1	+9.1	+5.4	+7.2	+1.8	+4.3
SimMTM	+33.5	+19.2	+5.1	-0.3	-0.3	-0.0	+3.0	+1.2	+0.5			
Ci	-1.9	-1.8	-0.7	+0.3	+0.3	+0.2	+13.7	-6.5	-0.5	+0.3	+0.0	+1.7
CiTrus (p)	+2.1	-3.3	-2.2	-0.9	-0.8	-0.1	-1.3	-6.1	+0.4	+5.1	-1.0	+1.5
CiTrus (fp)	+8.8	+1.1	+1.3	-0.8	+0.1	-0.0	+11.8	+1.2	+5.6	-22.1	-18.9	-9.3
CiTrus (mp)	+1.1	-4.8	-2.1	-1.2	-0.4	-0.3	+9.1	+3.0	-0.4	+0.1	-4.0	-1.8

Table 2: A comparison between a pre-trained and fine-tuned version of the model, and the same model trained from scratch on the downstream datasets. Each value is the average percentage improvement (across all three metrics) of pre-training compared to training from scratch. Values are made bold for the data regime within a dataset where pre-training and fine-tuning most increases the performance to show the effect of data availability on pre-training improvements.

signal transfer learning, it is a natural choice to look at convolutions. Convolutional networks have learnable filters that can learn representations in the frequency domain, and are good at capturing local features in the time series. We propose a model that combines the best of both worlds that we call CiTrus, a [C]onvolution-[Tr]ansformer hybrid, as shown in Figure 1b. The encoder in our model is a 3-layer residual convolutional network (a more detailed description of the convolutional network can be found in Appendix), and the transformer is a PatchTST (Nie et al. 2022) transformer. Our reason for choosing a PatchTST transformer, similar to bioFAME, is that it shows especially good performance for masked auto-encoding and is channel-independent. Channel-independence is important for transfer learning because when we pre-train the model on a certain number of channels, the transformer can easily handle a new number of channels in the downstream tasks. To create channel-independence for the convolutional encoder, we concatenate the number of channels along the batch, and both pre-train and fine-tune the model with a single channel as input. The pretrain head in our model is a convolutional decoder that has the same structure as the encoder, but flipped.

Similar to the earlier work, our model also uses masked autoencoding in pre-training. Normally, masked auto-encoding works with non-overlapping patches, but our convolutional encoder does not generate non-overlapping patches, and so we need to adapt the masking approach. Specifically, we use the output length of the convolutional encoder as the number of patches, and the output channels

as the feature dimension, which is mapped to a latent dimension by a linear layer. To perform masked auto-encoding, we need to define what part of the original signal was masked. Since convolutions contain information from neighboring activations and the receptive fields of neighboring patches overlap, patches have information about the original signal in a neighboring patch. This means that it could be easy for a neighboring patch of a masked patch to predict the original signal in the masked patch. Thus, masked auto-encoding becomes fairly trivial (depending on how much overlap there is in the two patches). To overcome this issue, we perform block masking, similar to Hubert (Hsu et al. 2021), where consecutive patches are masked at once. The number of consecutive patches is determined by the block size, and the total number of masked patches by the mask ratio. Our convolutional network is designed in such a way that the number of output patches is equal to the number of timesteps in the input signal divided by 8, and we create a correspondence between each output patch and a non-overlapping segment in the original signal of size 8. This allows us to calculate the reconstruction loss only with respect to the masked patches of the input signal. Although this is not perfect, since neighboring patches on either end of the block of masked patches can learn information about their neighbors, the issue of leaking information through neighbors is largely avoided with block masking.

Frequency pre-training (fp) Besides predicting the original input time-series signal, we can also push the model to explicitly predict frequency representations of the original

Dataset	EMG			ECG			PPG			HAR		
Data percentage	20%	50%	80%	0.5%	1%	2%	10%	20%	50%	10%	20%	50%
NLPatchTST	+17.3	+7.5	+6.0	+2.2	+3.6	+1.9	-0.5	-0.3	+1.6	-4.9	-3.7	-0.9
CiTrus	+6.3	+8.1	+3.1	+6.0	+3.8	+2.4	+1.1	+1.5	-0.6	-0.8	+0.2	-0.7
Dataset	FDB			Epilepsy			Gesture			SleepEDF		
Data percentage	0.5%	1%	2%	1%	5%	10%	10%	20%	50%	0.5%	1%	2%
NLPatchTST	-2.0	+0.1	-0.9	+0.1	+0.5	-0.1	+3.8	+1.9	+1.3	-5.5	-2.5	-2.5
CiTrus	-0.5	+0.5	-0.1	-0.2	+0.4	-0.1	+12.7	+11.1	-0.3	-4.7	-3.0	-3.2

Table 3: A comparison of multimodal pre-training to unimodal pre-training, where each value is the average improvement (across all three metrics) in percentages. Values that are larger than 0, indicating performance improvement, are made bold.

signal by predicting the spectrogram that corresponds to the masked patches instead of the original signal. The same low-frequencies can be repeated across patches, so to make the prediction of the spectrogram more challenging, we z-score the spectrograms along the time dimension. This new pre-training method is visualized in Figure 1b. Its exact settings and implementation are discussed in Appendix .

NLPatchTST In order to ablate the impact of the convolutional encoder, we develop a new model, by using a 3-layer multi-layer perceptron (MLP) to encode and decode each patch. We refer to this model as NLPatchTST (Non-Linear PatchTST) to differentiate from the original PatchTST model that uses a linear embedding layer.

Multimodal pre-training Given that the utility of multimodal pre-training was verified for the bioFAME model, we explore how well multimodal pre-training works for CiTrus. To pre-train CiTrus with multimodal data, each modality is passed through the convolutional encoder and transformer independently. This ensures that the convolutional encoder and transformer see data from both modalities and can learn to adapt its weights to both. This likely increases the versatility of the model because it learns jointly relevant features and representations. In our work we follow bioFAME and use two modalities, EEG and EOG, during pre-training, with a separate decoder for each modality. Specifically, the EEG and EOG signals are concatenated along the batch dimension in the convolutional encoder and transformer. After the transformer, the EEG and EOG context features are separated again, and concatenated along the latent dimension, see Figure 1c. The context features are then used as input for each decoder to predict the missing patches in each modality. During training we sample the patches independently for each modality, which allows information for a masked patch in one modality to be available from the other modality. This makes it easier to learn cross-modality information.

Transfer learning to new datasets Previous works, such as TPC and bioFAME transfer a pre-trained model to new downstream datasets with different temporal lengths by interpolating the data to match the signal length of the pre-training dataset. This causes a mismatch in sampling frequencies between the downstream fine-tuning datasets and the pre-train dataset. The potential frequency representation learned by the encoder and the temporal relationships learned by the transformer on the pre-training dataset are

now potentially irrelevant because they act on a completely different frequency range and timescale. We therefore propose a new strategy where the fine-tuning dataset is resampled to match the frequency of the pre-training dataset. This allows the model to attend to similar frequency spectra in the fine-tuning data as the pre-training data, and likely requires less ‘re-training’. If the length of the resampled fine-tuning data is now longer than the temporal length of the pre-training signal, we use an overlapping sliding window approach, and average the embeddings across the windows. If the length of the re-sampled fine-tuning data is shorter, we pad the signal with zeros.

Experiments

Evaluation framework & datasets Similar to previous work (Zhang et al. 2022), we use the SleepEDF, a large sleep EEG dataset (Kemp et al. 2000) for pre-training. The dataset consists of 30 second windows of EEG data sampled at 100Hz. For the uni-modal pre-training we use the two EEG channels that are captured. For the multi-modal pre-training we use the two EEG channels and the (single-channel) EOG data that is from the same dataset. As downstream datasets, we use 4 bio-signal datasets that were used to evaluate the TFC, bioFAME, and SimMTM models with:

- An electromyography (EMG) dataset (Goldberger et al. 2000) with a 375ms window length, sampled at 4KHz, and a single channel.
- A gesture recognition dataset (Liu et al. 2009) with a 3.15s window length, sampled at 100Hz, and 3 channels.
- An EEG Epilepsy dataset with a 1.02s window size, sampled at 174Hz, and a single channel.
- An electromotor fault-detection (FD-B) (Lessmeier et al. 2016) dataset with a 80ms window size, sampled at 64KHz, and a single channel.

Additionally, to increase the diversity of downstream tasks and modalities we test, we also add additional datasets:

- A photoplethysmography (PPG) dataset (Schmidt et al. 2018) with a 60s window length, sampled at 64Hz, and a single channel.
- The HAR dataset (Reyes-Ortiz et al. 2015) with a 2.56s window length, sampled at 50Hz, and 6 channels.
- An electrocardiogram (ECG) dataset (Moody 1983) with a 10s window length, sampled at 250Hz, and 2 channels.

Dataset	ECG			PPG			HAR			Gesture		
	0.5%	1%	2%	10%	20%	50%	10%	20%	50%	10%	20%	50%
PatchTST (s)	+4.5	-0.3	-0.7	+58.9	+60.0	+58.9	+23.9	+22.1	+19.7	+16.0	+18.5	+9.5
PatchTST (p)	+6.7	+10.1	+3.5	+52.9	+58.9	+57.8	+14.8	+17.2	+18.8	+3.7	+5.6	+4.2
bioFAME (s)	+5.2	+2.9	+2.6	+60.7	+55.9	+47.7	+16.7	+15.3	+16.0	+7.8	+10.9	+9.5
bioFAME (mp)	+15.4	+11.4	+9.8	+64.1	+47.8	+56.2	+14.6	+16.6	+26.5	-0.3	+2.1	+0.1
SimMTM (s)	+4.4	+15.3	+8.1	+30.1	+29.9	+51.9	+0.2	-0.1	-0.4	-3.8	+0.0	-1.7
SimMTM (p)	+1.4	+1.7	-1.8	+24.3	+26.9	+28.4	-0.3	-0.6	-0.1	-0.1	+0.6	-0.7
NLPatchTST (s)	-0.5	-2.0	-2.6	+49.6	+50.4	+64.3	+20.9	+20.7	+15.8	+8.8	+14.2	+3.0
NLPatchTST (p)	+3.3	+3.5	-0.5	+58.6	+55.9	+61.8	+17.1	+20.1	+18.6	-0.6	+3.8	+3.5
NLPatchTST (mp)	+5.5	+8.0	-0.2	+57.6	+52.5	+64.9	+10.6	+14.7	+18.8	+3.3	+6.4	+4.9
Ci (s)	+0.2	+3.8	+2.6	+29.1	+30.4	+20.4	+22.7	+17.8	+13.2	+8.2	+4.9	+2.7
Ci (p)	-1.2	+1.6	+2.9	+39.1	+41.7	+31.9	+18.5	+20.4	+11.7	+0.8	+3.9	+4.1
CiTrus (s)	+0.4	+6.0	+1.0	+32.1	+24.8	+21.1	+16.7	+18.7	+17.6	+21.1	+8.8	+3.7
CiTrus (p)	+6.7	+6.7	+8.6	+49.4	+51.0	+47.3	+19.3	+17.7	+14.3	-0.9	+0.5	+2.6
CiTrus (fp)	+0.5	+4.5	+3.1	+50.3	+48.1	+30.8	+11.5	+14.8	+17.7	+9.0	+2.8	+3.4
CiTrus (mp)	+11.0	+5.9	+8.0	+51.6	+49.7	+44.2	+17.4	+16.9	+14.2	+0.8	+6.9	+1.7

Table 4: A comparison between the previously used fine-tuning technique (temporal interpolation), and our proposed fine-tuning technique. Each value indicates the average performance improvement (across all three metrics) in percentages. Values larger than 0 are made bold.

- The SleepEDF test set

More information about these datasets can be found in Appendix .

The training, validation, and testing data splits were initially defined in the TFC work for the EMG, Gesture, FD-B, and Epilepsy datasets, and these splits were also used in bioFAME and SimMTM. Although we evaluate our proposed model on those previously defined data splits, see Appendix , we find that the variance in performance across test folds is much larger than across random seeds, see Table 6 in Appendix . Thus, to more comprehensively evaluate models used for transfer learning, we advocate for and implement a cross-validation procedure that averages test performance across 10-fold test splits. The training and validation data (the remaining 9 folds) is then reduced to the specific data-regime percentage. This leftover percentage of training and validation data is then split into 75% training and 25% validation data. Averaging the performance of the models across random seeds and test splits helps average out some of the performance’s randomness. We discuss the exact protocol we use to create the test splits in Appendix . For all the downstream tasks (except the SleepEDF test set), we follow the TFC work and split the data into 2 second windows before pre-training because the downstream data is often very short. For the SleepEDF evaluation, we keep the original 30s for pre-training. We also compare the performance regarding 30 vs 2 second windows in Appendix . Furthermore, we aim to understand the relationship between transfer learning and the amount of data available in the downstream datasets during fine-tuning. For this purpose, we evaluate each model across a range of data percentages during fine-tuning.

Experimental settings The implementations for the bioFAME, SimMTM, and PatchTST models are taken from their respective official implementations. The following are the model hyperparameters for all the models, except

SimMTM, for which we use the official implementation’s hyperparameters. The hyperparameters are matched to the bioFAME paper as much as possible to make the comparisons as fair as possible. We use a 4-layer transformer (with 64 latent dimensions, 128 feed-forward dimension and 8 heads), a 3-layer convolutional network (with 32 channels in the first residual convolution layer that double every layer, only applicable for CiTrus), a patch size of 20, a 0.5 masking ratio, and a block masking size of 5 (only applicable for CiTrus). All models are pre-trained for 200 epochs with a 128 batch size, and a 0.0001 learning rate. All models are fine-tuned for 100 epochs with a 64 batch size, without any augmentations, and the same learning rate as during pre-training. All hyperparameters were kept the same during development. Our models are pre-trained and fine-tuned on an AWS instance with 4 NVIDIA A10 GPUs, with [42, 1337, 1212, 9999] as the model seeds, and 42 as the seed for data randomization and fold generation. Given the 10 data folds, there are 40 runs per model, per data regime and per dataset. For a deeper explanation of the model settings see Appendix . Since the evaluation is done on classification tasks, we report the accuracy (ACC), area under the curve of the receiver operating characteristic (ROC), and area under the precision-recall curve (PRC) to get a variety of classification metrics. Lastly, standard deviations and Wilcoxon signed-rank test outcomes for each experiment are discussed in Appendix .

Model architecture comparisons First, we evaluate how a variety of model architectures perform on the transfer tasks. The PatchTST, bioFAME, SimMTM are evaluated and compared to our NLPatchTST and CiTrus models. To understand the effect the transformer in our model has on the performance, we also compare Ci, which uses just the encoded features in our proposed model, to CiTrus. For each dataset, except the EMG and FD-B, we use our proposed

sliding window approach during fine-tuning, which generally results in the best performance especially for the baselines we test against. The EMG and FD-B datasets have windows for predictions that are too short to use the sliding window technique with, so we interpolate the data to 200 timesteps as described in the TFC work. Moreover, to limit the size of the table, we report the hardest data regime; the lowest amount of data available for each dataset. The percentage of training + validation data that is available is mentioned after the name of the dataset in Table 1. Note, since the convolutional encoder used in SimMTM model only works with inputs that are 200 samples in length, it is not compatible with the SleepEDF test set, so we do not report the result.

The results in Table 1 indicate that convolution-based models (SimMTM, Ci, and CiTrus) almost always achieve the best performance. For ECG, PPG, and FD-B, using the context features from CiTrus performs better than using the encoded features. The CiTrus model with pre-training and fine-tuning performs the best on those datasets as well. For every dataset except the Gesture dataset, the CiTrus model is atleast in the top three best models. The fact that both the HAR and Gesture datasets are accelerometer-based datasets could explain the lower performance on these datasets. Our frequency-based pre-training model performs the best on average, see Appendix .

Training from scratch vs pre-training To understand the effect of pre-training on downstream performance, we calculate how much better each model performs after pre-training. Since we use three metrics in Table 1 to evaluate each approach, we calculate the average percentage improvement across the three metrics, with respect to training the model from scratch. We also highlight the largest improvement across the data regimes for each model and each dataset in Table 2.

For most settings in Table 2 pre-training improves downstream performance, but this improvement does depend on the dataset and the underlying structure of the model. Specifically, for the EMG dataset we can see dramatic increases in performance for transformer-based models across all data regimes. Whereas gains for the Ci model, which is fully convolutional, are marginal. Moreover, for the Gesture, PPG, and SleepEDF datasets pre-training improves performance the most for the lowest data regime.

Multimodal vs unimodal pre-training For both the CiTrus and the NLPatchTST model we investigate whether multimodal pre-training further improves performance over unimodal pre-training. Similar to the pre-training results, we compute the average percentage improvement across the three metrics with respect to uni-modal pre-training. In this case we bold results that improve performance over unimodal pre-training in Table 3.

There are a few datasets where multimodal pre-training almost always performs better: the EMG, ECG, and Gesture datasets. These show clear improvements for multimodal pre-training. Moreover, the CiTrus model generally benefits more from multi-modal pre-training than the NLPatchTST model. This could be due to the inherent ability of convolu-

tional networks to learn local feature representations jointly across multiple modalities. Interestingly, for the SleepEDF test set, multimodal pre-training degrades performance, potentially because the fine-tuning is an EEG-only task.

Resampling-adaptive fine-tuning

To verify how well our proposed fine-tuning approach works for new datasets with different temporal lengths, sampling frequencies, and modalities, we compare it to the interpolation method used in the TFC, bioFAME, and SimMTM works. For each model, we compute the average percentage improvement that is achieved by using our proposed fine-tuning technique as compared to temporal interpolation. For this experiment we select datasets that have very different sampling frequencies than the original pre-training dataset. We exclude the EMG and FD-B datasets, since their length are extremely short ($< 400ms$), and lead to very small temporal samples (< 40) at 100Hz.

In Table 4 the average percentage increase in metrics shows that in almost all cases our new fine-tuning approach markedly improves performance. Especially on the PPG dataset the new approach reaches improvements of 64%. Moreover, improvements are achieved for both convolutional and transformer-based models. Pre-trained models benefit the most from our fine-tuning approach.

Discussion

In this work we assessed the transferability of neural networks pre-trained on a large EEG dataset and fine-tuned on low-data downstream bio-signal datasets. First, we generally find that models with convolutions (Ci and CiTrus) perform the best. We believe this is largely due to their inductive bias and parameter efficiency. Convolutions share many of their weights when processing the timeseries, and given that convolutions are learnable frequency filters, they transfer well to datasets where features come from similar parts of the frequency spectrum. Second, the idea that the parameter efficiency and inductive bias of convolutions is key in low-data settings is further supported by the fact that transformer-based models improve the most with pre-training, especially in low-data settings, which indicates that they require more data to learn the important temporal relationships required for predictions. This is also true for other types of data, such as images, where the vision transformer (ViT) (Dosovitskiy et al. 2020) famously starts outperforming convolutions when trained with a large dataset. Third, multimodal pre-training often improves downstream fine-tuning performance even more. Fourth, we find that pre-training is not necessary for the EMG and FD-B datasets. Although the TFC, bioFAME, and SimMTM models found bio-signal datasets to transfer well to FD-B, which is an electromotor dataset, we find that our well-tuned CNN outperforms any other model when trained from scratch. Additionally, datasets where performance is already high, like the Epilepsy dataset, do not benefit much from pre-training either. Fifth, we developed CiTrus, which combines a CNN encoder with a transformer, and its frequency-based pre-trained version performs the best on average across datasets

for the lowest and highest data regimes we tested. Lastly, our fine-tuning approach is better in essentially all cases for all models, and improves performance up to 60%. Our approach improves performance the most for pre-trained models, which we believe is because the temporal relationships the encoder and transformer learn are now aligned between the pre-training and downstream datasets.

References

- Andrzejak, R. G.; Lehnertz, K.; Mormann, F.; Rieke, C.; David, P.; and Elger, C. E. 2001. Indications of nonlinear deterministic and finite-dimensional structures in time series of brain electrical activity: Dependence on recording region and brain state. *Physical Review E*, 64(6): 061907.
- Buitinck, L.; Louppe, G.; Blondel, M.; Pedregosa, F.; Mueller, A.; Grisel, O.; Niculae, V.; Prettenhofer, P.; Gramfort, A.; Grobler, J.; Layton, R.; VanderPlas, J.; Joly, A.; Holt, B.; and Varoquaux, G. 2013. API design for machine learning software: experiences from the scikit-learn project. In *ECML PKDD Workshop: Languages for Data Mining and Machine Learning*, 108–122.
- Casselman, J.; Onopa, N.; and Khansa, L. 2017. Wearable healthcare: Lessons from the past and a peek into the future. *Telematics and Informatics*, 34(7): 1011–1023.
- Charlton, P. H.; Celka, P.; Farukh, B.; Chowienczyk, P.; and Alastruey, J. 2018. Assessing mental stress from the photoplethysmogram: a numerical study. *Physiological measurement*, 39(5): 054001.
- Chien, H.-Y. S.; Goh, H.; Sandino, C. M.; and Cheng, J. Y. 2022. Maeeg: Masked auto-encoder for eeg representation learning. *arXiv preprint arXiv:2211.02625*.
- Deldari, S.; Spathis, D.; Malekzadeh, M.; Kawsar, F.; Salim, F.; and Mathur, A. 2023. Latent Masking for Multimodal Self-supervised Learning in Health Timeseries. *arXiv preprint arXiv:2307.16847*.
- Dong, J.; Wu, H.; Zhang, H.; Zhang, L.; Wang, J.; and Long, M. 2024. Simmtm: A simple pre-training framework for masked time-series modeling. *Advances in Neural Information Processing Systems*, 36.
- Dosovitskiy, A.; Beyer, L.; Kolesnikov, A.; Weissenborn, D.; Zhai, X.; Unterthiner, T.; Dehghani, M.; Minderer, M.; Heigold, G.; Gelly, S.; et al. 2020. An image is worth 16x16 words: Transformers for image recognition at scale. *arXiv preprint arXiv:2010.11929*.
- Durongbhan, P.; Zhao, Y.; Chen, L.; Zis, P.; De Marco, M.; Unwin, Z. C.; Venneri, A.; He, X.; Li, S.; Zhao, Y.; et al. 2019. A dementia classification framework using frequency and time-frequency features based on EEG signals. *IEEE Transactions on Neural Systems and Rehabilitation Engineering*, 27(5): 826–835.
- Eldele, E.; Ragab, M.; Chen, Z.; Wu, M.; Kwok, C.-K.; Li, X.; and Guan, C. 2023. Self-supervised contrastive representation learning for semi-supervised time-series classification. *IEEE Transactions on Pattern Analysis and Machine Intelligence*.
- Foumani, N. M.; Mackellar, G.; Ghane, S.; Irtza, S.; Nguyen, N.; and Salehi, M. 2024. Eeg2rep: enhancing self-supervised EEG representation through informative masked inputs. *arXiv preprint arXiv:2402.17772*.
- Goldberger, A. L.; Amaral, L. A.; Glass, L.; Hausdorff, J. M.; Ivanov, P. C.; Mark, R. G.; Mietus, J. E.; Moody, G. B.; Peng, C.-K.; and Stanley, H. E. 2000. PhysioBank, PhysioToolkit, and PhysioNet: components of a new research resource for complex physiologic signals. *circulation*, 101(23): e215–e220.
- Gong, L.; Li, M.; Zhang, T.; and Chen, W. 2023. EEG emotion recognition using attention-based convolutional transformer neural network. *Biomedical Signal Processing and Control*, 84: 104835.
- Guibas, J.; Mardani, M.; Li, Z.; Tao, A.; Anandkumar, A.; and Catanzaro, B. 2021. Adaptive fourier neural operators: Efficient token mixers for transformers. *arXiv preprint arXiv:2111.13587*.
- He, K.; Chen, X.; Xie, S.; Li, Y.; Dollár, P.; and Girshick, R. 2022. Masked autoencoders are scalable vision learners. In *Proceedings of the IEEE/CVF conference on computer vision and pattern recognition*, 16000–16009.
- Hsu, W.-N.; Bolte, B.; Tsai, Y.-H. H.; Lakhotia, K.; Salakhutdinov, R.; and Mohamed, A. 2021. Hubert: Self-supervised speech representation learning by masked prediction of hidden units. *IEEE/ACM transactions on audio, speech, and language processing*, 29: 3451–3460.
- Kemp, B.; Zwinderman, A. H.; Tuk, B.; Kamphuisen, H. A.; and Obery, J. J. 2000. Analysis of a sleep-dependent neuronal feedback loop: the slow-wave microcontinuity of the EEG. *IEEE Transactions on Biomedical Engineering*, 47(9): 1185–1194.
- Lessmeier, C.; Kimotho, J. K.; Zimmer, D.; and Sextro, W. 2016. Condition monitoring of bearing damage in electromechanical drive systems by using motor current signals of electric motors: A benchmark data set for data-driven classification. In *PHM Society European Conference*, volume 3.
- Li, Y.; Li, X.; Ratcliffe, M.; Liu, L.; Qi, Y.; and Liu, Q. 2011. A real-time EEG-based BCI system for attention recognition in ubiquitous environment. In *Proceedings of 2011 international workshop on Ubiquitous affective awareness and intelligent interaction*, 33–40.
- Li, Z.; Kovachki, N.; Azizzadenesheli, K.; Liu, B.; Bhattacharya, K.; Stuart, A.; and Anandkumar, A. 2020. Fourier neural operator for parametric partial differential equations. *arXiv preprint arXiv:2010.08895*.
- Liu, J.; Zhong, L.; Wickramasuriya, J.; and Vasudevan, V. 2009. uWave: Accelerometer-based personalized gesture recognition and its applications. *Pervasive and Mobile Computing*, 5(6): 657–675.
- Liu, R.; Zippi, E. L.; Pouransari, H.; Sandino, C.; Nie, J.; Goh, H.; Azemi, E.; and Moin, A. 2023. Frequency-aware masked autoencoders for multimodal pretraining on biosignals. *arXiv preprint arXiv:2309.05927*.

- McFee, B.; Raffel, C.; Liang, D.; Ellis, D. P.; McVicar, M.; Battenberg, E.; and Nieto, O. 2015. librosa: Audio and music signal analysis in python. In *SciPy*, 18–24.
- Miltiadous, A.; Gionanidis, E.; Tzimourta, K. D.; Gianakeas, N.; and Tzallas, A. T. 2023. DICE-net: a novel convolution-transformer architecture for Alzheimer detection in EEG signals. *IEEE Access*.
- Moody, G. 1983. A new method for detecting atrial fibrillation using RR intervals. *Proc. Comput. Cardiol.*, 10: 227–230.
- Neyshabur, B.; Sedghi, H.; and Zhang, C. 2020. What is being transferred in transfer learning? *Advances in neural information processing systems*, 33: 512–523.
- Nie, Y.; Nguyen, N. H.; Sinthong, P.; and Kalagnanam, J. 2022. A time series is worth 64 words: Long-term forecasting with transformers. *arXiv preprint arXiv:2211.14730*.
- Odinaka, I.; Lai, P.-H.; Kaplan, A. D.; O’Sullivan, J. A.; Sirevaag, E. J.; Kristjansson, S. D.; Sheffield, A. K.; and Rohrbaugh, J. W. 2010. ECG biometrics: A robust short-time frequency analysis. In *2010 IEEE International Workshop on Information Forensics and Security*, 1–6. IEEE.
- Peh, W. Y.; Yao, Y.; and Dauwels, J. 2022. Transformer convolutional neural networks for automated artifact detection in scalp EEG. In *2022 44th Annual International Conference of the IEEE Engineering in Medicine & Biology Society (EMBC)*, 3599–3602. IEEE.
- Reyes-Ortiz, J.; Anguita, D.; Oneto, L.; and Parra, X. 2015. Smartphone-based recognition of human activities and postural transitions data set. *UCI Machine Learning Repository. School Inf. Comput. Sci. Univ. California at Irvine, Irvine, CA, USA, available online: <http://archive.ics.uci.edu/ml/datasets/Smartphone-Based+Recognition+of+Human+Activities+and+Postural+Transitions>*.
- Schmidt, P.; Reiss, A.; Duerichen, R.; Marberger, C.; and Van Laerhoven, K. 2018. Introducing wesad, a multimodal dataset for wearable stress and affect detection. In *Proceedings of the 20th ACM international conference on multimodal interaction*, 400–408.
- Song, Y.; Zheng, Q.; Liu, B.; and Gao, X. 2022. EEG conformer: Convolutional transformer for EEG decoding and visualization. *IEEE Transactions on Neural Systems and Rehabilitation Engineering*, 31: 710–719.
- Weiderpass, H.; Pachi, C.; Yamamoto, J.; Hamamoto, A.; Onodera, A.; and Sacco, I. 2013. Time-frequency analysis methods for detecting effects of diabetic neuropathy. *International Journal for Numerical Methods in Biomedical Engineering*, 29(9): 1000–1010.
- Xu, M. A.; Moreno, A.; Wei, H.; Marlin, B. M.; and Rehg, J. M. 2023. Retrieval-Based Reconstruction For Time-series Contrastive Learning. *arXiv preprint arXiv:2311.00519*.
- Yang, C.; Westover, M.; and Sun, J. 2024. Biot: Biosignal transformer for cross-data learning in the wild. *Advances in Neural Information Processing Systems*, 36.
- Zhang, H.; Cisse, M.; Dauphin, Y. N.; and Lopez-Paz, D. 2017. mixup: Beyond empirical risk minimization. *arXiv preprint arXiv:1710.09412*.
- Zhang, X.; Zhao, Z.; Tsiligkaridis, T.; and Zitnik, M. 2022. Self-supervised contrastive pre-training for time series via time-frequency consistency. *Advances in Neural Information Processing Systems*, 35: 3988–4003.

Appendices

K-fold generation

The K-fold generation is split into two strategies, based on how the original test split was defined. For the EMG, FD-B, Epilepsy, and Gesture datasets, which were used in (Zhang et al. 2022), the data was concatenated. Then, a StratifiedKfold object was instantiated (Buitinck et al. 2013), with 10 folds, shuffling, and its random state set to 42. This splits the data into 10 folds, and we take each split as a test fold once. The remaining 9 folds are used as a training + validation set. Then, depending on the data regime, we use stratified train_test_split() to only keep X% of the training + validation data, with random_state=42. This is to simulate specific data regimes, X here refers to the percentages used in the main text and the rest of the Appendix. Lastly, we perform a stratified split to split the leftover training + validation data into a training and validation set, with 75% of the remaining data in the training set, and random_state=42. The only difference in this strategy for the other datasets: HAR, ECG, and PPG, is that they are split into a training, validation, and test set based on the subject the windows come from. Thus, to ensure the folds reflect subjects instead of just doing a stratified split across the windows. For the ECG and PPG dataset, we instantiate a KFold object with 10 folds, and for HAR (because there are multiple timeseries per subject) we instantiate a GroupKFold object. Then, for the ECG and PPG datasets, the subjects are split into 10 folds, for the HAR dataset, the timeseries are split, based on the subjects as groups, into 10 splits. The rest of the procedure is the same as before, except that stratification in case of leaving X% of the data is done based on both subject and label, i.e. we keep each class and subject in the leftover training + validation dataset atleast once. For the SleepEDF dataset we do not create 10-fold splits to fine-tune on because of time limits. Namely, each split would require a complete pre-training cycle, which are costly in terms of time. Thus, the results for the SleepEDF fine-tuning are averaged only over the random seeds.

Results on pre-defined splits from TFC paper

The following table, Table 5, shows the performance of the models on the original (single) test split. The models are pre-trained and fine-tuned in the way described in our main text. Since we find that resampling to 30s after pre-training on 30s windows performs the best for the EMG and FD-B datasets, when we use a resampling/interpolation technique, see Appendix , we use the models pre-trained on 30s windows in the SleepEDF dataset, similar to the BioFAME paper. Then, the fine-tuning dataset is resampled to 30s (3000 timesteps) based on the method used in (Liu et al. 2023), linear interpolation. This method only deviates for the SimMTM and CiTrus (fp) models because the SimMTM model does not accept 30s inputs, and the CiTrus (fp) model performs better with 2s inputs. SimMTM (Dong et al. 2024) follows the original TFC paper (Zhang et al. 2022) by pre-training on 2s splits, and the SimMTM (s) is the same model architecture as TFC trained from scratch. Lastly, for the Gesture and Epilepsy datasets, the data is simply padded to 200 timesteps (from 178) for the Epilepsy dataset, and resampled (from 206) to 200 for the Gesture dataset, and the models pre-trained on 2s (200 timesteps) splits of the SleepEDF dataset are used. This is done because both dataset’s temporal length is almost the same as the 2s pre-training windows (200 timesteps). For the BioFAME model, we find the same performance within the standard deviation reported in the original paper for the EMG dataset. However, for the FD-B and Epilepsy datasets the performance is slightly lower than the original paper. This may be because we do not use any label augmentations, such as MixUp (Zhang et al. 2017) during the fine-tuning stage. For the SimMTM paper we find the same performance, except on the EMG dataset. Generally, we tried to match our framework as closely as possible to bioFAME and SimMTM, but since they each use different pre-training lengths, it can be hard to exactly replicate the reported performances.

Dataset	EMG			FD-B			Epilepsy			Gesture		
Metric	ACC	ROC	PRC	ACC	ROC	PRC	ACC	ROC	PRC	ACC	ROC	PRC
PatchTST (s)	95.12	98.06	98.79	69.16	57.41	43.57	93.89	50.25	80.35	61.67	71.18	40.96
PatchTST (p)	94.51	<u>99.54</u>	<u>99.15</u>	68.8	57.53	43.51	<u>95.47</u>	50.24	80.35	62.5	70.42	40.56
bioFAME (s)	<u>95.73</u>	<u>99.33</u>	97.14	71.48	57.96	44.19	89.62	50.24	80.37	46.46	70.41	38.7
bioFAME (mp)	98.17	99.88	99.85	70.4	57.77	43.93	93.76	50.24	80.36	55.42	71.84	40.47
NLPatchTST (s)	<u>95.73</u>	97.88	98.67	74.69	58.54	44.72	93.05	50.26	80.37	62.71	72.56	41.65
NLPatchTST (p)	95.12	98.96	<u>99.36</u>	79.08	59.18	45.48	95.11	50.25	80.36	63.96	73.27	42.55
NLPatchTST (mp)	95.12	98.33	98.92	69.73	57.84	43.87	<u>95.51</u>	50.25	80.37	63.54	72.4	41.8
SimMTM (s)	92.68	97.24	91.11	62.66	57.03	41.14	93.2	50.25	80.37	<u>78.75</u>	<u>73.2</u>	45.59
SimMTM (p)	95.12	98.52	96.39	77.68	59.07	43.73	95.46	50.26	80.37	79.79	72.95	<u>44.61</u>
Ci (s)	95.12	98.49	98.58	<u>82.9</u>	<u>59.98</u>	46.51	95.32	50.26	80.38	61.88	<u>73.12</u>	<u>42.7</u>
Ci (p)	<u>96.95</u>	98.64	98.48	69.5	58.91	45.51	94.11	<u>50.26</u>	80.38	60.83	72.31	42.14
CiTrus (s)	93.9	98.18	98.17	84.13	60.03	<u>46.5</u>	95.28	<u>50.27</u>	<u>80.38</u>	<u>65.63</u>	71.54	40.92
CiTrus (p)	95.12	98.38	98.45	80.93	59.53	45.7	90.28	50.27	80.38	65.21	72.31	41.16
CiTrus (fp)	54.27	76.11	72.11	30.84	53.11	36.88	56.54	49.99	80.23	38.54	60.53	32.32
CiTrus (mp)	<u>95.73</u>	98.87	96.69	<u>81.79</u>	<u>59.68</u>	<u>45.89</u>	95.55	50.25	80.37	62.29	71.96	40.85

Table 5: The performance of each model we use in this paper (trained by us) on the original test splits as defined in (Zhang et al. 2022). The best performing models are made bold, second best are double-underlined, and third best are single-underlined.

Frequency pre-training settings

Instead of predicting the masked signal in the original window, for the frequency pre-training strategy, the masked autoencoder model predicts the masked parts of the spectrogram instead. To create the spectrogram from the pre-training data, we use Librosa's melspectrogram function (McFee et al. 2015). Specifically, when pre-training on SleepEDF with 2s windows, the spectrogram is generated with a hop_length of 4, 200 ffts, 64 mels, $f_{min} = 0$, $f_{max} = 20$, centering, and a window length of 60. We add 40 to the mel spectrogram and then divide them by 40. For the 2s pre-training, we only use the first 25 spectrogram timesteps (26 are generated in total) because that corresponds to the number of patches after the convolutional encoder $200/8 = 25$. Lastly, the mel spectrograms are z-scored along the time dimension to push the model to focus on frequency content in the spectrograms that are masked that is not available in the other spectrograms. For the 30s window pre-training setting, we use a hop_length of 8, 1024 ffts, 128 mels, and a window length of 60. All other settings are the same. In this case we obtain 376 timesteps, and since we have $3000/8 = 375$ patches after the convolutional encoder, we only use the first 375.

Result variance across seeds and folds

To verify that it is important to cross-validate transfer learning models for bio-signals, we evaluated how much the performance of each model fluctuates both across folds and across seeds. The variance across random seeds evaluates how models differ in their final solution with different starting and training stochasticity. The variance across test folds evaluates how the model performs with differences in the training and test distributions. Given that we are especially interested in low-data regimes, the variance in test folds can be very high. For example, we can get lucky and select a really good 1% of the dataset as our training and validation set that represents the test set well. With only 1% of the data, the chance that the training and validation set do not represent the test set well is much higher than it is when we use more data in our training and validation set. In Table 6 we see that variance across folds is markedly higher than it is across random seeds, sometimes leading to almost 5000% more variance than seen across random seeds. The way we calculate the values is that we take the variance across test folds, average it across the three metrics, and divide it by the average variance across the random seeds and subtract 1 from that result, and multiply it by 100 to get a percentage. This gives us the percentage increase in variance.

Dataset	EMG			ECG			PPG			HAR		
Data	20%	50%	80%	0.5%	1%	2%	10%	20%	50%	10%	20%	50%
PatchTST (s)	+53	+404	+136	+1488	+1496	+4319	+1713	+440	+197	+101	+384	+393
PatchTST (p)	+121	+40	+86	+998	+4608	+1905	+290	+974	+137	+119	+144	+380
bioFAME (s)	+71	+152	+112	+2311	+3478	+3745	+816	+497	+208	+475	+210	+187
bioFAME (mp)	+96	+154	+73	+2218	+2290	+3199	+421	+374	+391	+35	+20	+178
NLPatchTST (s)	+45	+28	+251	+1010	+1894	+2246	+420	+367	+86	+258	+498	+827
NLPatchTST (p)	+21	+53	+165	+1097	+1086	+1613	+231	+417	+148	+115	+131	+618
NLPatchTST (mp)	+124	+66	+229	+1785	+2252	+2087	+419	+319	+148	+117	+190	+706
SimMTM (s)	+88	+123	+100	+1082	+454	+1608	+850	+237	+479	+555	+732	+429
SimMTM (p)	-56	+238	+66	+725	+827	+1903	+206	+494	+562	+506	+556	+439
Ci (s)	+1018	+703	+684	+2402	+1369	+2479	+488	+526	+298	+916	+1564	+1627
Ci (p)	+251	+191	+268	+2179	+3485	+2269	+625	+682	+564	+793	+1431	+1084
CiTrus (s)	+104	+559	+137	+2162	+1068	+1638	+113	+149	+212	+205	+342	+1088
CiTrus (p)	-15	+100	+250	+1923	+1114	+1518	+346	+423	+294	+142	+737	+750
CiTrus (fp)	+89	+110	+424	+365	+320	+354	+18	+15	+45	+398	+192	+100
CiTrus (mp)	+129	+117	+174	+763	+3840	+1347	+255	+193	+309	+104	+882	+887
Dataset	FDB			Epilepsy			Gesture			SleepInference		
Data	0.5%	1%	2%	1%	5%	10%	10%	20%	50%	0.5%	1%	2%
PatchTST (s)	+71	+252	+41	+85	+102	+261	+339	+320	+379			
PatchTST (p)	+42	+189	+44	+20	+89	+234	+143	+231	+549			
bioFAME (s)	+238	+132	+181	+103	+171	+260	+137	+499	+618			
bioFAME (mp)	+217	+213	+29	+37	+16	+154	+61	+34	+22			
NLPatchTST (s)	+77	+83	+59	-12	-24	+13	+253	+439	+426			
NLPatchTST (p)	+57	+54	+26	+26	+43	+180	+258	+219	+447			
NLPatchTST (mp)	+109	+161	+112	+101	+99	+239	+199	+290	+220			
SimMTM (s)	+49	+9	+68	+22	+146	+169	+902	+168	+460			
SimMTM (p)	+120	+119	+175	+226	+192	+164	+350	+262	+219			
Ci (s)	+337	+268	+190	+36	+215	+419	+214	+231	+344			
Ci (p)	+420	+230	+31	+226	+188	+376	+54	+256	+475			
CiTrus (s)	+469	+161	+70	+134	+50	+256	+99	+245	+255			
CiTrus (p)	+105	-22	-25	+8	+67	+150	+148	+89	+248			
CiTrus (fp)	+25	+232	+17	+7	+109	+92	+14	+71	+74			
CiTrus (mp)	+112	+7	+37	+20	+8	+131	+129	+126	+112			

Table 6: The percentage increase in variance across test folds compared to the variance across models for the same test fold. The percentage increase is averaged across all metrics. All percentages larger than 0 are made bold.

The following few tables provide the standard deviation in our results, both for every data regime (low, middle, and high), but also for our results on pre-training, reported in Table 2, multimodal pre-training, reported in Table 3, and our fine-tuning approach, reported in Table 4.

Low-data regime results standard deviations

Dataset	EMG@20%			ECG@0.5%			PPG@10%			HAR@10%		
Metric	ACC	ROC	PRC	ACC	ROC	PRC	ACC	ROC	PRC	ACC	ROC	PRC
PatchTST (s)	8.59	11.1	11.15	11.71	1.94	17.44	7.96	6.31	7.12	4.58	2.89	4.9
PatchTST (p)	11.2	11.94	13.38	13.27	2.22	17.45	7.46	7.71	9.12	5.02	2.42	3.95
bioFAME (s)	9.08	13.04	10.56	7.92	1.6	18.44	5.98	4.24	5.91	5.28	2.2	3.47
bioFAME (mp)	8.35	6.91	10.62	11.47	2.89	18.15	7.11	5.16	7.04	5.86	3.18	5.34
NLPatchTST (s)	13.32	8.99	10.99	14.6	1.22	17.61	8.51	7.42	7.46	5.17	2.69	4.97
NLPatchTST (p)	11.7	7.33	10.21	14.66	2.02	17.55	6.22	6.19	7.04	6.1	2.67	5.37
NLPatchTST (mp)	10.81	6.54	9.66	14.42	2.0	17.4	6.89	5.9	6.8	5.37	2.51	4.6
SimMTM (s)	21.42	10.76	15.44	17.71	2.19	17.08	10.77	9.55	12.36	5.75	2.64	5.15
SimMTM (p)	6.43	17.95	14.01	15.16	1.98	17.39	10.78	10.59	14.06	4.19	2.39	4.78
Ci (s)	4.47	2.25	5.25	17.11	3.67	17.43	8.27	7.79	7.47	3.34	2.64	4.78
Ci (p)	5.29	2.19	4.99	17.89	3.13	17.23	7.54	7.7	7.69	6.46	2.8	5.62
CiTrus (s)	4.85	1.13	1.18	15.4	3.7	17.37	7.76	8.57	9.45	4.63	2.47	4.96
CiTrus (p)	8.04	4.41	7.47	18.86	3.1	17.42	6.72	8.21	8.67	4.7	2.67	5.31
CiTrus (fp)	3.93	3.38	3.73	11.84	4.26	17.51	8.3	9.24	11.74	5.02	2.64	4.83
CiTrus (mp)	6.17	1.4	4.67	16.94	3.43	17.74	5.85	6.24	6.32	5.43	2.82	5.63
Dataset	FDB@0.5%			Epilepsy@1%			Gesture@10%			SleepInference@0.5%		
Metric	ACC	ROC	PRC	ACC	ROC	PRC	ACC	ROC	PRC	ACC	ROC	PRC
PatchTST (s)	3.1	1.64	1.19	1.42	4.04	2.3	7.68	3.64	7.24	0.92	0.35	0.51
PatchTST (p)	2.92	1.84	1.35	1.06	2.3	1.32	8.11	3.34	7.08	1.28	0.75	0.96
bioFAME (s)	3.94	1.99	1.3	1.8	1.76	0.82	7.33	4.81	5.73	0.39	0.58	0.65
bioFAME (mp)	5.05	2.83	2.24	1.71	1.0	0.4	7.79	6.03	7.55	2.07	0.46	0.81
NLPatchTST (s)	5.84	2.37	1.59	4.5	9.69	4.85	9.28	4.45	7.9	2.22	1.09	1.18
NLPatchTST (p)	2.37	1.76	1.26	1.16	3.31	2.1	7.88	4.31	7.94	1.03	0.53	1.07
NLPatchTST (mp)	2.59	1.98	1.57	1.5	3.72	2.34	6.49	3.72	7.05	2.29	0.81	1.21
SimMTM (s)	7.45	2.68	2.56	3.19	0.24	1.36	9.09	4.1	8.09	0.0	0.0	0.0
SimMTM (p)	12.16	5.89	4.66	0.92	0.32	1.34	7.68	3.23	7.1	0.0	0.0	0.0
Ci (s)	8.19	2.97	3.33	2.07	0.73	0.32	7.53	6.02	8.27	1.52	0.43	0.68
Ci (p)	6.7	3.12	3.44	0.92	0.69	0.28	7.19	4.22	6.73	1.1	0.53	0.64
CiTrus (s)	7.89	3.45	3.73	1.84	0.95	0.51	7.32	4.43	6.83	2.25	0.62	0.76
CiTrus (p)	4.82	2.08	2.85	1.34	4.15	2.53	8.47	4.51	7.79	0.78	0.26	0.82
CiTrus (fp)	5.71	2.13	2.47	1.8	1.18	0.59	7.18	4.81	7.51	5.31	2.18	2.3
CiTrus (mp)	3.77	2.41	2.82	1.0	4.38	2.82	6.7	3.85	6.71	3.3	1.14	1.62

Table 7: The standard-deviations across both seeds and folds for the low-data regime.

Middle-data regime results standard deviations

Dataset	EMG@50%			ECG@1%			PPG@20%			HAR@20%		
Metric	ACC	ROC	PRC	ACC	ROC	PRC	ACC	ROC	PRC	ACC	ROC	PRC
PatchTST (s)	12.55	10.73	14.25	15.05	2.41	16.76	8.16	5.08	6.27	3.86	2.66	4.8
PatchTST (p)	12.75	13.02	14.71	14.13	2.62	17.38	8.9	6.47	7.21	5.59	2.7	5.01
bioFAME (s)	12.44	14.84	15.79	9.84	2.48	18.09	8.12	3.64	4.03	4.5	2.58	3.88
bioFAME (mp)	7.14	3.52	7.57	12.26	2.96	18.31	7.94	4.48	7.11	6.47	3.02	5.59
NLPatchTST (s)	7.97	4.23	6.94	15.43	2.15	16.99	10.96	6.36	8.68	4.84	2.86	5.85
NLPatchTST (p)	5.76	2.88	5.18	16.64	2.17	17.09	7.47	6.34	7.27	5.49	2.74	5.42
NLPatchTST (mp)	10.13	4.3	7.02	15.92	2.38	17.46	8.74	5.16	6.25	6.46	2.55	5.11
SimMTM (s)	6.51	3.09	7.08	13.0	3.31	17.14	10.41	8.04	10.97	5.35	3.04	5.8
SimMTM (p)	8.78	6.8	9.31	15.76	3.22	16.96	9.74	8.29	10.78	4.12	3.1	5.86
Ci (s)	3.26	2.34	5.42	15.92	3.49	16.88	7.6	6.39	7.56	3.11	2.69	5.03
Ci (p)	5.03	1.64	3.38	18.42	3.5	16.74	8.24	7.22	7.99	6.26	2.88	5.61
CiTrus (s)	3.27	1.28	0.86	16.79	3.85	17.2	7.36	6.14	6.28	4.53	2.68	4.62
CiTrus (p)	4.84	1.56	4.16	20.0	3.59	17.01	9.04	8.25	8.66	4.2	2.64	5.33
CiTrus (fp)	4.09	1.49	3.47	12.01	4.3	17.53	7.04	7.4	9.59	6.5	2.53	4.46
CiTrus (mp)	5.61	3.28	5.7	17.04	3.89	17.12	8.89	7.09	7.88	4.9	2.85	5.57
Dataset	FDB@1%			Epilepsy@5%			Gesture@20%			SleepInference@1%		
Metric	ACC	ROC	PRC	ACC	ROC	PRC	ACC	ROC	PRC	ACC	ROC	PRC
PatchTST (s)	5.96	2.46	2.07	0.7	0.89	0.4	7.19	3.63	7.79	1.94	0.37	0.25
PatchTST (p)	3.4	1.64	1.36	0.85	0.96	0.55	6.83	2.62	5.51	1.74	0.25	0.43
bioFAME (s)	4.59	2.7	2.01	0.79	0.71	0.25	8.53	4.81	8.06	0.84	0.12	0.13
bioFAME (mp)	4.04	2.51	2.2	0.86	0.68	0.26	8.04	4.13	8.58	2.22	0.29	0.61
NLPatchTST (s)	4.86	2.44	2.4	5.52	14.84	7.48	7.54	3.91	8.05	2.58	0.45	0.35
NLPatchTST (p)	4.43	2.2	2.01	1.07	2.18	1.29	7.13	2.69	6.61	0.26	0.17	0.43
NLPatchTST (mp)	4.15	2.6	2.07	0.86	1.73	0.96	6.8	2.93	5.91	1.42	0.23	0.6
SimMTM (s)	12.55	5.6	5.26	0.68	0.18	1.38	5.56	1.99	4.31	0.0	0.0	0.0
SimMTM (p)	1.7	1.28	1.18	0.84	0.25	1.19	4.73	2.06	4.08	0.0	0.0	0.0
Ci (s)	2.96	1.02	1.23	0.82	0.5	0.24	7.11	3.06	7.41	1.14	0.16	0.43
Ci (p)	3.01	1.21	2.14	0.65	0.42	0.19	7.33	3.32	7.2	0.84	0.23	0.3
CiTrus (s)	4.72	1.1	2.19	0.88	0.6	0.3	6.78	2.39	5.69	0.56	0.16	0.43
CiTrus (p)	3.8	1.92	2.79	0.77	1.69	1.14	7.19	2.85	6.87	1.34	0.15	0.3
CiTrus (fp)	1.29	1.25	1.61	0.68	0.44	0.23	8.91	3.63	8.12	8.14	4.16	3.31
CiTrus (mp)	3.56	1.54	2.31	0.83	1.5	1.1	6.13	2.81	5.63	1.59	0.24	0.6

Table 8: The standard-deviations across both seeds and folds for the middle-data regime.

High-data regime results standard deviations

Dataset	EMG@80%			ECG@2%			PPG@50%			HAR@50%		
Metric	ACC	ROC	PRC	ACC	ROC	PRC	ACC	ROC	PRC	ACC	ROC	PRC
PatchTST (s)	6.95	2.87	5.52	14.31	2.6	17.13	7.41	4.52	5.49	3.84	2.58	4.91
PatchTST (p)	8.47	6.85	9.51	15.6	2.39	17.18	6.52	5.21	6.87	4.07	2.66	5.04
bioFAME (s)	8.81	5.66	9.0	7.79	2.2	18.31	5.76	3.45	4.46	5.22	2.56	4.42
bioFAME (mp)	6.98	2.79	5.69	8.34	2.96	18.41	6.2	7.37	9.98	4.48	2.91	5.27
NLPatchTST (s)	5.99	1.77	4.32	17.17	2.76	17.69	7.98	4.69	7.25	3.28	2.53	4.93
NLPatchTST (p)	5.18	2.92	6.23	15.65	2.08	17.54	5.87	4.38	6.12	3.29	2.74	5.49
NLPatchTST (mp)	6.13	3.21	7.26	14.15	2.48	17.8	4.31	4.14	5.19	3.73	2.63	5.03
SimMTM (s)	5.93	1.45	3.51	17.75	2.79	16.67	10.27	7.74	11.1	4.61	2.53	5.13
SimMTM (p)	6.91	2.27	3.9	16.9	2.17	16.41	8.94	7.63	10.79	4.08	2.66	5.29
Ci (s)	3.05	1.46	3.45	20.55	3.7	17.0	6.72	5.75	7.89	2.41	2.51	4.54
Ci (p)	3.9	1.61	2.93	14.74	3.77	17.77	5.75	6.05	7.66	3.73	2.58	4.74
CiTrus (s)	3.67	1.02	0.7	14.44	3.87	17.24	7.48	6.66	10.59	2.78	2.6	5.01
CiTrus (p)	3.51	1.88	2.31	16.83	3.95	17.35	5.75	7.17	8.31	3.05	2.59	5.08
CiTrus (fp)	3.32	0.99	0.84	10.68	4.33	17.59	6.31	6.42	9.48	4.28	2.59	4.88
CiTrus (mp)	3.94	1.29	3.01	14.7	3.89	17.65	5.65	5.76	8.13	3.3	2.69	5.27
Dataset	FDB@2%			Epilepsy@10%			Gesture@50%			SleepInference@2%		
Metric	ACC	ROC	PRC	ACC	ROC	PRC	ACC	ROC	PRC	ACC	ROC	PRC
PatchTST (s)	4.68	2.27	2.42	0.77	0.79	0.31	6.92	3.04	7.71	1.01	0.19	0.26
PatchTST (p)	3.24	1.92	1.76	0.77	0.94	0.5	7.44	2.66	6.82	1.76	0.53	0.59
bioFAME (s)	4.32	2.4	2.44	0.88	0.66	0.23	8.37	3.56	8.52	0.94	0.25	0.31
bioFAME (mp)	2.26	1.61	2.13	0.69	0.5	0.22	7.42	3.31	7.57	2.89	0.72	1.16
NLPatchTST (s)	3.48	2.28	2.51	4.51	5.43	3.22	6.43	3.51	7.73	2.73	0.98	0.92
NLPatchTST (p)	4.02	2.31	2.33	0.74	0.81	0.38	7.84	2.86	7.81	0.88	0.09	0.17
NLPatchTST (mp)	2.49	1.87	1.87	0.8	0.84	0.37	7.8	3.18	7.51	1.32	0.4	0.73
SimMTM (s)	2.67	1.16	1.18	0.39	0.29	1.09	5.04	2.11	5.21	0.0	0.0	0.0
SimMTM (p)	1.45	1.14	1.18	0.59	0.24	0.8	5.07	1.75	3.84	0.0	0.0	0.0
Ci (s)	2.52	1.13	1.14	0.88	0.32	0.1	5.72	2.56	5.88	2.75	0.44	0.41
Ci (p)	2.18	1.14	1.11	0.73	0.31	0.13	7.05	2.79	5.7	0.92	0.12	0.12
CiTrus (s)	4.27	1.2	1.91	0.78	0.35	0.12	5.84	2.47	5.4	1.0	0.49	0.8
CiTrus (p)	3.85	1.51	2.17	0.84	0.52	0.3	7.05	2.85	7.53	1.52	0.35	0.61
CiTrus (fp)	1.69	1.16	1.66	0.61	0.36	0.14	10.78	3.07	8.8	5.61	1.83	2.25
CiTrus (mp)	3.14	1.42	1.85	0.78	0.91	0.69	5.81	2.81	5.82	1.22	0.73	1.22

Table 9: The standard-deviations across both seeds and folds for the high-data regime.

Pre-training results standard deviations

Dataset	EMG			ECG			PPG			HAR		
Data	20%	50%	80%	0.5%	1%	2%	10%	20%	50%	10%	20%	50%
PatchTST	13.2	13.0	12.8	4.4	4.2	3.8	6.0	4.8	6.4	4.4	3.7	2.8
bioFAME	12.8	10.3	14.1	4.1	3.6	3.0	4.7	5.2	8.5	4.4	4.0	4.5
NLPatchTST (p)	15.1	15.3	15.3	4.4	4.8	4.6	6.0	5.9	6.9	3.8	4.2	2.2
NLPatchTST (mp)	13.2	11.7	14.4	4.8	4.4	3.9	5.6	6.6	7.1	3.7	4.5	2.0
Ci	14.6	10.1	5.4	4.3	4.5	5.3	5.2	5.1	5.3	3.5	3.1	1.5
CiTrus (p)	12.8	10.3	5.9	5.2	4.8	4.1	8.8	7.4	9.1	4.6	2.7	1.7
CiTrus (fp)	15.1	7.7	5.5	5.3	5.8	4.9	11.2	8.7	8.9	4.0	4.2	2.2
CiTrus (mp)	14.6	9.6	6.6	5.2	3.8	4.1	8.5	7.0	8.4	4.7	2.5	1.9

Dataset	FDB			Epilepsy			Gesture			SleepInference		
Data	0.5%	1%	2%	1%	5%	10%	10%	20%	50%	0.5%	1%	2%
PatchTST	2.0	1.8	1.4	2.5	0.9	0.8	6.2	5.1	4.4	1.0	0.6	0.9
bioFAME	1.7	1.6	0.9	1.5	0.6	0.4	7.0	6.2	6.3	1.4	1.0	1.5
NLPatchTST (p)	1.9	2.0	1.3	6.6	9.3	4.4	6.6	5.4	4.6	1.7	1.1	1.4
NLPatchTST (mp)	2.3	2.0	1.3	6.6	9.6	4.3	6.5	5.1	4.3	2.2	1.1	1.1
Ci	1.9	1.6	1.4	1.0	0.4	0.3	7.4	4.5	3.6	1.5	1.0	1.2
CiTrus (p)	1.5	1.5	1.2	3.1	1.3	0.6	7.7	6.1	5.2	1.7	0.7	1.3
CiTrus (fp)	2.0	1.6	1.8	1.5	0.6	0.4	8.0	6.6	6.9	3.7	5.3	3.8
CiTrus (mp)	2.4	1.7	1.3	3.1	1.3	0.8	6.6	4.6	4.1	2.5	0.8	1.5

Table 10: The standard-deviations across both seeds and folds in the average performance improvement results when pre-training in Table 2.

Multi-modal pre-training results standard deviations

Dataset	EMG			ECG			PPG			HAR		
Data	20%	50%	80%	0.5%	1%	2%	10%	20%	50%	10%	20%	50%
NLPatchTST	32.0	22.8	20.5	7.6	12.3	7.4	9.6	9.2	9.4	6.0	5.6	2.3
CiTrus	17.1	17.1	8.8	25.4	15.5	8.4	9.4	11.7	8.6	4.9	2.9	2.2

Dataset	FDB			Epilepsy			Gesture			SleepInference		
Data	0.5%	1%	2%	1%	5%	10%	10%	20%	50%	0.5%	1%	2%
NLPatchTST	4.2	2.9	1.7	3.1	1.6	0.6	11.3	6.4	6.6	1.6	1.5	1.2
CiTrus	4.0	2.8	2.5	3.5	1.6	0.8	17.6	11.7	7.8	4.0	1.6	2.7

Table 11: The standard-deviations across both seeds and folds in the average performance improvement results with multimodal pre-training in Table 3.

Fine-tuning approach results standard deviations

Dataset	ECG			PPG			HAR			Gesture		
	0.5%	1%	2%	10%	20%	50%	10%	20%	50%	10%	20%	50%
Data	15.5	11.1	8.2	28.7	31.1	26.6	7.0	6.2	4.2	24.2	13.4	9.4
PatchTST (s)	13.9	18.1	9.6	28.1	30.3	27.5	8.9	7.8	5.4	10.5	8.4	7.9
PatchTST (p)	13.1	10.1	8.4	37.5	30.3	22.2	7.3	6.1	6.1	17.2	12.0	10.7
bioFAME (s)	20.6	13.2	12.2	31.8	24.2	35.4	7.3	7.0	5.6	15.6	9.8	10.1
bioFAME (mp)	17.1	17.8	14.3	28.7	24.0	39.2	3.3	2.5	2.4	6.4	5.8	4.4
SimMTM (s)	12.6	9.7	12.3	28.7	24.8	25.4	1.7	1.5	1.9	13.0	3.8	3.3
SimMTM (p)	10.6	9.5	8.7	22.2	30.5	27.5	6.8	6.6	4.0	18.4	13.4	7.0
NLPatchTST (s)	13.6	16.0	12.9	26.6	39.1	27.6	7.6	7.1	5.6	8.6	6.8	7.7
NLPatchTST (p)	12.5	21.9	8.3	25.5	33.3	28.3	7.6	7.6	5.9	9.8	8.5	8.1
NLPatchTST (mp)	11.9	12.8	13.6	15.9	27.5	20.8	6.9	4.9	3.6	30.9	8.8	7.7
Ci (s)	11.9	20.4	17.8	20.0	32.4	24.0	6.2	5.5	4.5	12.8	7.5	7.1
Ci (p)	9.5	18.5	8.1	23.5	25.7	19.9	8.6	4.9	3.8	33.1	10.2	6.6
CiTrus (s)	33.8	25.5	25.7	29.6	29.4	31.8	6.8	4.9	4.6	15.2	8.0	7.6
CiTrus (p)	6.1	18.8	8.9	24.7	24.4	23.7	4.8	6.9	4.9	13.3	7.8	6.7
CiTrus (fp)	44.1	22.3	20.3	27.5	31.6	29.6	7.7	5.4	4.0	10.0	8.6	6.8
CiTrus (mp)												

Table 12: The standard-deviations across both seeds and folds in the average performance improvement results when using our fine-tuning approach in Table 4.

Average model results

The following table, Table 13, shows the average performance of each model across the datasets. The results are shown for each metric, and for each data regime. Generally, the best-performing models are variants of our proposed model architectures. Especially CiTrus (fp), and CiTrus (mp) perform really well for the low-data regime. CiTrus (fp) clearly performs the best for the high data regime. For the middle data regime, the best model is Ci (s).

Data regime	Low			Middle			High		
Metric	ACC	ROC	PRC	ACC	ROC	PRC	ACC	ROC	PRC
PatchTST (s)	60.79	71.31	56.97	67.48	76.89	63.82	73.88	79.65	68.49
PatchTST (p)	63.63	73.25	59.02	67.39	75.83	62.46	73.1	78.76	67.05
bioFAME (s)	58.58	70.52	54.84	63.0	74.54	59.52	68.05	77.59	63.1
bioFAME (mp)	64.04	75.54	60.89	67.85	77.5	63.73	73.33	79.46	67.23
NLPatchTST (s)	60.86	72.01	58.5	68.77	75.89	64.01	74.71	79.53	68.8
NLPatchTST (p)	66.18	75.78	61.94	70.82	78.13	65.94	76.04	80.12	69.35
NLPatchTST (mp)	65.99	75.71	61.7	70.66	77.99	65.47	75.93	80.13	69.21
Ci (s)	71.9	78.45	<u>66.39</u>	78.37	81.19	70.33	80.21	<u>82.4</u>	<u>72.42</u>
Ci (p)	70.94	78.7	<u>65.74</u>	76.12	<u>80.72</u>	69.19	<u>80.78</u>	<u>82.04</u>	<u>71.96</u>
CiTrus (s)	71.52	<u>78.53</u>	66.08	<u>77.15</u>	<u>80.65</u>	<u>69.37</u>	<u>80.68</u>	82.0	<u>72.1</u>
CiTrus (p)	<u>71.93</u>	78.28	65.78	<u>75.89</u>	80.18	<u>68.81</u>	80.38	81.81	71.7
CiTrus (fp)	73.01	78.1	<u>66.18</u>	<u>76.8</u>	80.36	69.08	82.6	82.52	72.91
CiTrus (mp)	<u>72.71</u>	<u>78.69</u>	66.42	76.67	80.19	<u>69.22</u>	80.28	81.4	71.15

Table 13: A comparison of the different model architectures on average across the datasets for each data regime. The best result for each metric is shown in bold, the second best result is double-underlined, and the third best result is single-underlined.

Experimental statistics

To statistically verify the experiments in the main paper, we perform a one-sided Wilcoxon statistical test. For Table 14 we compare each model’s performance to our CiTrus (fp) model and compute whether our model is significantly better. The statistical test is a verification of the results shown in Table 1. In most cases our model performs significantly better than many of the baselines, and for the EMG, ECG, PPG, and FD-B datasets the performance of the CiTrus (fp) is statistically better than almost all models. Then, in Table 15, 16, and 17 we verify the significance of the other three experiments in the main text, and find that in most cases where we see improvements, the new method is also significantly better.

Dataset	EMG@20%			ECG@0.5%			PPG@10%			HAR@10%		
Metric	ACC	ROC	PRC	ACC	ROC	PRC	ACC	ROC	PRC	ACC	ROC	PRC
PatchTST (s)	9e-13	9e-13	9e-13	9e-13	9e-13	8e-11	2e-04	4e-04	1e-05	1.0	1.0	0.93
PatchTST (p)	9e-13	2e-12	9e-13	3e-10	2e-12	2e-10	5e-04	4e-04	4e-05	5e-06	1e-07	2e-09
bioFAME (s)	9e-13	2e-12	9e-13	2e-12	9e-13	9e-13	7e-05	8e-04	7e-05	2e-12	9e-13	9e-13
bioFAME (mp)	9e-13	2e-09	3e-10	5e-09	3e-12	9e-12	4e-05	4e-02	7e-03	3e-05	5e-02	2e-03
NLPatchTST (s)	9e-13	5e-11	9e-13	9e-13	9e-13	4e-11	1e-05	2e-06	4e-08	1.0	1.0	0.98
NLPatchTST (p)	9e-13	1e-07	4e-08	1e-10	2e-11	2e-10	3e-04	4e-03	1e-04	0.64	0.79	0.14
NLPatchTST (mp)	3e-08	9e-12	9e-12	3e-10	4e-11	5e-10	7e-05	1e-03	3e-05	2e-06	8e-06	9e-08
SimMTM (s)	9e-13	9e-13	9e-13	8e-11	7e-08	2e-08	2e-05	0.09	0.07	1.0	1.0	1.0
SimMTM (p)	9e-13	9e-13	9e-13	9e-12	2e-09	4e-08	1e-07	2e-03	1e-03	1.0	1.0	1.0
Ci (s)	0.06	0.06	0.09	2e-10	2e-04	5e-06	6e-04	2e-06	2e-06	1.0	1.0	1.0
Ci (p)	2e-04	3e-03	2e-03	4e-10	3e-06	2e-05	2e-05	1e-04	3e-06	1.0	1.0	1.0
CiTrus (s)	2e-02	0.38	0.51	6e-09	4e-02	4e-03	6e-04	2e-04	3e-03	1.0	1.0	1.0
CiTrus (p)	4e-06	8e-04	3e-05	3e-09	5e-08	3e-07	0.08	1e-02	4e-02	1.0	1.0	1.0
CiTrus (mp)	5e-06	2e-02	3e-04	1e-07	5e-04	2e-02	0.13	2e-02	5e-03	1.0	1.0	1.0
Dataset	FDB@0.5%			Epilepsy@1%			Gesture@10%			SleepInference@0.5%		
Metric	ACC	ROC	PRC	ACC	ROC	PRC	ACC	ROC	PRC	ACC	ROC	PRC
PatchTST (s)	9e-13	9e-13	9e-13	1e-02	2e-05	2e-04	5e-05	0.09	1e-04	1.0	1.0	1.0
PatchTST (p)	3e-12	9e-13	9e-13	0.08	7e-06	1e-05	0.17	0.97	0.7	1.0	1.0	1.0
bioFAME (s)	9e-13	9e-13	9e-13	7e-03	0.93	1.0	9e-13	4e-10	3e-12	1.0	1.0	1.0
bioFAME (mp)	3e-12	9e-13	9e-13	6e-03	1.0	1.0	2e-09	5e-03	3e-08	1.0	1.0	1.0
NLPatchTST (s)	9e-13	9e-13	9e-13	9e-13	9e-13	9e-13	3e-05	0.47	2e-04	1.0	1.0	1.0
NLPatchTST (p)	6e-12	2e-12	9e-13	7e-04	2e-08	2e-08	5e-02	0.98	0.7	1.0	1.0	1.0
NLPatchTST (mp)	2e-11	2e-12	9e-13	7e-03	5e-07	7e-06	0.64	0.99	0.91	1.0	1.0	1.0
SimMTM (s)	9e-13	2e-12	2e-12	0.83	9e-13	9e-13	0.83	1.0	1.0			
SimMTM (p)	2e-08	2e-09	3e-11	0.12	9e-13	9e-13	1.0	1.0	1.0			
Ci (s)	5e-06	8e-04	1e-03	0.86	1.0	1.0	4e-08	2e-06	3e-08	1.0	1.0	1.0
Ci (p)	7e-08	5e-08	2e-09	1.0	1.0	1.0	3e-08	0.07	2e-07	1.0	1.0	1.0
CiTrus (s)	1e-07	3e-07	5e-09	0.09	1.0	1.0	1e-05	0.24	2e-03	1.0	1.0	1.0
CiTrus (p)	5e-07	3e-10	5e-12	0.98	0.87	0.94	2e-06	4e-02	1e-03	1.0	1.0	1.0
CiTrus (mp)	5e-07	3e-09	1e-10	1.0	0.35	0.16	2e-02	0.93	0.6	1.0	1.0	1.0

Table 14: The p-value for the one-sided Wilcoxon signed-rank test across seeds and folds. Significant values are made bold, and indicate that improvements in Table 1 are significant. The comparisons are all done compared to our CiTrus (fp) model, with the one-sided assumption that CiTrus (fp)’s performance is higher.

Dataset	EMG			ECG			PPG			HAR		
Data	20%	50%	80%	0.5%	1%	2%	10%	20%	50%	10%	20%	50%
PatchTST	0.67	0.66	0.67	0.44	2e-02	0.18	0.8	4e-02	0.98	2e-08	2e-10	2e-04
bioFAME	0.52	0.24	8e-04	3e-04	2e-05	3e-08	0.92	0.17	0.3	1e-08	5e-07	9e-12
NLPatchTST (p)	0.17	7e-05	3e-06	0.43	0.28	0.44	2e-03	0.45	0.78	4e-03	2e-05	3e-02
NLPatchTST (mp)	3e-04	2e-07	3e-07	0.06	0.68	0.73	3e-03	0.84	0.19	2e-07	5e-09	5e-05
Ci	2e-02	3e-06	0.35	0.36	0.08	0.64	0.85	0.3	0.07	2e-12	3e-08	0.16
CiTrus (p)	0.07	1e-05	8e-06	0.05	0.56	0.45	2e-02	0.66	0.39	0.08	7e-05	0.28
CiTrus (fp)	7e-04	2e-03	4e-02	1e-08	3e-07	5e-08	1e-03	2e-03	8e-03	3e-08	9e-04	0.73
CiTrus (mp)	0.77	2e-02	3e-02	0.62	0.99	1e-02	9e-03	0.54	0.44	0.43	6e-05	5e-03

Dataset	FDB			Epilepsy			Gesture			SleepInference		
Data	0.5%	1%	2%	1%	5%	10%	10%	20%	50%	0.5%	1%	2%
PatchTST	0.42	0.11	0.94	4e-02	0.75	6e-03	7e-05	2e-05	4e-03	2e-12	0.12	0.12
bioFAME	0.08	3e-02	3e-05	0.43	0.77	2e-02	2e-04	2e-04	1e-04	0.47	0.88	0.62
NLPatchTST (p)	2e-04	2e-05	2e-03	3e-11	5e-11	3e-11	4e-03	3e-03	1e-02	2e-12	0.12	0.12
NLPatchTST (mp)	0.56	4e-05	0.54	1e-10	4e-12	1e-09	3e-06	1e-05	6e-04	2e-12	0.12	0.12
Ci	0.09	4e-05	1e-04	7e-03	7e-06	1e-06	2e-03	5e-06	0.87	4e-04	0.88	0.12
CiTrus (p)	0.15	4e-02	6e-03	2e-02	0.68	0.13	0.37	1e-04	0.7	2e-12	0.12	0.88
CiTrus (fp)	0.17	2e-03	1e-05	0.18	8e-03	0.3	2e-05	0.25	9e-03	2e-12	0.12	0.12
CiTrus (mp)	0.52	0.42	0.44	3e-05	0.12	0.14	2e-04	2e-02	0.95	0.18	0.12	0.62

Table 15: The p-value for the one-sided Wilcoxon signed-rank test for accuracy values across seeds and folds. Significant values are made bold, and indicate that improvements in Table 2 are significant.

Dataset	EMG			ECG			PPG			HAR		
Data	20%	50%	80%	0.5%	1%	2%	10%	20%	50%	10%	20%	50%
NLPatchTST	2e-02	0.12	0.21	3e-02	0.17	0.21	0.55	0.42	0.1	6e-06	3e-04	8e-04
CiTrus	0.06	3e-03	3e-03	0.23	0.64	4e-02	0.96	0.51	0.72	0.13	0.26	4e-02

Dataset	FDB			Epilepsy			Gesture			SleepInference		
Data	0.5%	1%	2%	1%	5%	10%	10%	20%	50%	0.5%	1%	2%
NLPatchTST	3e-03	0.88	4e-03	0.28	0.15	5e-03	3e-03	0.09	0.5	2e-12	0.12	0.12
CiTrus	0.45	0.36	0.16	0.14	0.38	0.69	9e-06	9e-07	0.81	4e-12	0.38	0.25

Table 16: The p-value for the one-sided Wilcoxon signed-rank test for accuracy values across seeds and folds. Significant values are made bold, and indicate that improvements in Table 3 are significant.

Dataset	ECG			PPG			HAR			Gesture		
Data	0.5%	1%	2%	10%	20%	50%	10%	20%	50%	10%	20%	50%
PatchTST (s)	0.53	0.31	0.12	2e-12	2e-10	2e-12	2e-12	2e-12	2e-12	5e-04	5e-07	5e-05
PatchTST (p)	0.07	1e-03	0.07	2e-12	2e-10	2e-12	3e-11	5e-08	2e-12	0.06	3e-03	2e-02
bioFAME (s)	2e-02	3e-02	6e-03	2e-12	5e-12	2e-12	2e-12	5e-12	2e-12	0.06	5e-05	3e-04
bioFAME (mp)	3e-08	6e-11	2e-11	2e-12	1e-07	2e-12	9e-12	2e-12	2e-12	0.37	0.17	0.69
SimMTM (s)	0.2	9e-09	1e-03	1e-06	1e-06	2e-07	0.83	0.23	0.69	1e-04	0.97	0.09
SimMTM (p)	0.52	0.11	0.5	3e-03	1e-05	3e-07	2e-02	0.12	0.4	0.29	0.37	0.35
NLPatchTST (s)	0.93	0.3	0.15	8e-08	3e-07	2e-12	4e-12	2e-12	2e-12	5e-02	3e-06	3e-02
NLPatchTST (p)	0.99	0.29	0.13	2e-12	1e-11	2e-12	2e-12	2e-12	2e-12	0.68	1e-03	5e-03
NLPatchTST (mp)	0.06	0.11	0.52	2e-12	1e-10	2e-12	1e-10	9e-12	2e-12	6e-03	3e-03	8e-04
Ci (s)	0.14	0.24	0.37	5e-08	2e-07	4e-06	2e-12	2e-12	2e-12	0.72	3e-03	0.16
Ci (p)	0.48	0.39	0.48	2e-12	4e-10	2e-12	4e-12	2e-12	2e-12	0.29	0.33	2e-03
CiTrus (s)	0.95	0.11	0.6	3e-11	2e-07	4e-08	2e-12	2e-12	2e-12	1e-03	2e-04	0.08
CiTrus (p)	0.4	0.2	0.13	2e-12	9e-12	4e-12	2e-12	2e-12	2e-12	0.56	0.98	0.21
CiTrus (fp)	0.57	0.69	2e-02	2e-12	2e-12	7e-08	2e-12	4e-12	2e-12	7e-04	3e-02	1e-02
CiTrus (mp)	0.07	0.32	2e-02	2e-12	7e-10	2e-12	2e-12	2e-12	2e-12	0.23	2e-05	0.8

Table 17: The p-value for the double-sided Wilcoxon signed-rank test for accuracy values across seeds and folds. Significant values are made bold, and indicate that improvements in Table 4 are significant.

2 second or 30 second pre-training

The following table shows the percentage improvement of using 30 second pre-training windows for the SleepEDF dataset, and interpolating the size of the dataset to 3000 timesteps. Using 30s windows for pre-training is described in the bioFAME paper (Liu et al. 2023), whereas using 2s windows and resampling the fine-tuning datasets to 200 timesteps is described in the TFC paper (Zhang et al. 2022). Clearly, for the FD-B and EMG datasets, using longer pre-training data and resampling to those longer pre-training inputs improves performance. The same is true for PPG, although the improvements are less than using our sliding-window approach, as shown in Table 4. Although the long pre-training and resampling is sometimes better for the ECG datasets, this is only the case for model architectures that are outperformed by the other model architectures, as shown in Table 1, for example. For the Gesture and HAR datasets the long pre-training and resampling does not seem to improve performance, and in many cases even slightly degrades performance.

Dataset	ECG			PPG			HAR		
Data	0.5%	1%	2%	10%	20%	50%	10%	20%	50%
PatchTST (s)	+15.1	+3.2	+1.7	+42.8	+51.5	+50.6	+2.1	+2.1	+5.3
PatchTST (p)	+18.1	+19.4	+10.7	+22.5	+42.7	+46.2	+10.2	+10.2	+10.4
bioFAME (s)	+12.2	+7.2	+8.1	+59.3	+56.7	+47.0	+2.4	-6.4	-6.0
bioFAME (mp)	+32.6	+21.2	+16.3	+51.1	+52.4	+60.0	+8.9	-3.6	+12.5
NLPatchTST (s)	+2.0	-6.1	-3.2	+33.1	+36.2	+50.4	-0.5	+2.2	+4.7
NLPatchTST (p)	+14.1	+15.9	+12.4	+35.0	+42.1	+60.7	+3.8	+6.5	+1.9
NLPatchTST (mp)	+22.1	+24.7	+14.1	+40.5	+47.6	+60.4	+4.0	+6.9	+5.6
Ci (s)	-3.3	-2.6	-3.0	+20.3	+31.0	+17.4	-7.7	-3.9	-2.1
Ci (p)	-1.5	-1.9	-2.9	+38.2	+40.1	+32.1	-6.9	-6.4	-8.8
CiTrus (s)	-6.2	-2.3	-6.1	+19.0	+21.9	+17.6	-5.6	+1.9	+4.0
CiTrus (p)	+5.5	+6.6	+5.6	+36.5	+44.8	+45.8	-4.8	-6.2	-4.7
CiTrus (fp)	-15.6	-12.5	-14.1	+6.6	+6.6	+2.7	-21.0	-24.2	-23.5
CiTrus (mp)	+14.9	+8.0	+6.6	+39.5	+40.6	+45.8	-5.6	-5.8	-2.8

Dataset	Gesture			FDB			EMG		
Data	10%	20%	50%	0.5%	1%	2%	20%	50%	80%
PatchTST (s)	-18.4	-17.9	-9.6	+9.9	+20.8	+15.5	+85.7	+22.0	+6.0
PatchTST (p)	-7.9	-9.0	-6.1	+11.1	+17.7	+16.5	+60.6	+43.7	+20.4
bioFAME (s)	+33.5	+22.1	+18.5	+24.0	+27.2	+23.0	+70.9	+34.4	+14.7
bioFAME (mp)	+0.9	+4.6	+6.7	+21.7	+22.0	+14.9	+27.1	+15.3	+10.8
NLPatchTST (s)	-21.7	-20.9	-10.3	+13.4	+19.3	+13.2	+41.3	+10.1	+3.6
NLPatchTST (p)	-9.1	-8.7	-3.7	+21.7	+24.7	+23.3	+28.4	+8.5	+3.6
NLPatchTST (mp)	-10.3	-5.7	-4.0	+14.0	+16.8	+15.3	+22.7	+10.1	+5.4
Ci (s)	-21.7	-35.3	-10.1	+7.6	+4.2	+4.2	+1.7	+1.1	+0.4
Ci (p)	-29.2	-28.6	-9.2	+9.0	+6.3	+3.5	+2.9	+1.4	+0.6
CiTrus (s)	-18.7	-23.6	-17.8	+12.1	+6.9	+5.4	+0.3	+0.2	-0.1
CiTrus (p)	+0.7	-1.7	-5.6	+1.0	+4.7	+3.6	+5.5	+0.3	+0.0
CiTrus (fp)	-35.0	-38.1	-29.2	-5.1	-3.2	-0.8	-7.2	-9.8	-6.3
CiTrus (mp)	-4.1	-1.3	-2.0	+6.9	+7.4	+5.6	+2.9	+2.3	+0.6

Table 18: A comparison between using 2s windows from the SleepEDF pre-training dataset and resampling the fine-tuning dataset to 200 timesteps as described in (Zhang et al. 2022), and using 30s windows from the SleepEDF pre-training dataset, as described in (Liu et al. 2023), and resampling the fine-tuning dataset to 3000 timesteps. Each value indicates the average performance improvement (across all three metrics) in percentages. Values larger than 0 are made bold.

Exact data parameters

The Epilepsy, Gesture, EMG, and FD-B datasets are from the TFC paper (Zhang et al. 2022).

The link to their code: — <https://github.com/mims-harvard/TFC-pretraining/tree/main>

To download and pre-process the ECG, HAR, and PPG datasets, we based our code on (Xu et al. 2023).

The link to their code: — <https://github.com/maxxu05/rebar>

The script to download and pre-process the specific subset of the SleepEDF data is based on (Eldele et al. 2023).

The link to their code: — <https://gist.github.com/emadeldeen24/a22691e36759934e53984289a94cb09b>

SleepEDF The SleepEDF dataset (Eldele et al. 2023) contains 197 whole-night sleep recordings. It records two EEG channels (Fpz-Cz and Pz-Oz), an EOG channel, a respiratory (oro-nasal), an EMG channel located below the skin, and rectal temperature during each night of sleep. Similar to (Eldele et al. 2023; Liu et al. 2023), we use the cassette study, which is a subset of the dataset, that focuses on healthy caucasian subjects. Each 30 seconds in the final, preprocessed dataset, is associated with one of five sleeping stages: Rapid Eye Movement (REM), Non-rapid eye movement (N1, N2, N3), and Wake (W).

Epilepsy The Epilepsy dataset (Andrzejak et al. 2001) contains single-channel recordings from 500 subjects. Each time window that is labeled corresponds to 1 second, sampled at 178Hz, and is thus 178 timesteps long. In total, there are 11,500 samples with two classes: whether a subject is having a seizure in that 1-second time window or not.

Gesture The gesture dataset (Liu et al. 2009) contains 3-dimensional accelerometer data that exemplify 8 different hand gestures. Each time window corresponds to a specific gesture, and is 2.06seconds long. Although the sampling frequency is not clear (Zhang et al. 2022), it is assumed to be 100Hz, which is a common sampling frequency for accelerometer datasets like this. This means each sample is 206 timesteps long. The eight gestures in the datasets are: swiping left, swiping right, swiping up, swiping down, waving counterclockwise, waving clockwise, waving in a square, and waving in a right arrow.

EMG The EMG dataset (Goldberger et al. 2000) contains data from three different patients, a patient with neuropathy, myopathy, and a healthy volunteer. The timeseries from each subject is split into 1500 timestep windows, sampled at 4kHz the time windows correspond to 375ms of data. The label for each time window is the subject it came from. The goal is thus to classify whether the observed EMG in a specific time window is from someone suffering from neuropathy, myopathy, or a healthy volunteer.

FD-B The FD-B dataset (Lessmeier et al. 2016) is a fault detection dataset generated by an electromechanical drive system that monitors the rolling bearings. Each time window corresponds to a different fault in the electromotor. Specifically, the three classes are that a rolling is undamaged, inner damaged, and outer damaged. The data has a single channel, and is separated into time windows using a 5120 timestep sliding window, with a sampling frequency of 64kHz, each time window corresponds to 80ms.

ECG The ECG dataset (Moody 1983) contains dual channel electrocardiogram recordings, where each 10-second time-window, with a 250Hz sampling frequency, corresponds to 2500 time points. Each time window is either labeled as atrial fibrillation or a normal heart rhythm.

PPG The PPG dataset (Schmidt et al. 2018) contains single-channel photoplethysmogram recordings to perform affect detection. Each time window is one minute long, with a 64Hz sampling frequency, this corresponds to 3840 time steps. The possible labels for each time window are baseline, stress, amusement, and meditation.

HAR The HAR dataset (Reyes-Ortiz et al. 2015) contains 3-dimensional accelerometer and gyroscopic sensor data to classify daily activities. The total number of channels in the data is 6, and each labeled time window is 2.56s long, with a 50Hz sampling frequency, this corresponds to 128 timesteps. There are 6 labels; walking, walking upstairs, walking downstairs, sitting, standing, and laying.

Exact model parameters

Residual blocks in the convolutional encoder Each layer in the convolutional encoder is a residual block. One path through the residual block is a single convolution layer, with a kernel size of 3, a stride of 2, and a padding of 1, that increases the number of input channels C to $2*C$. The other path are two sequential convolutional layers, both with a kernel size of 3. The first convolutional layer has a stride of 1, and a padding of 1, without the bias parameters, and increases the number of input channels C to $2*C$. The second convolutional layer has a stride of 2, and a padding of 1, also without the bias parameters, and does not increase the number of channels further. The first convolutional layer is followed by 1D BatchNorm, a GELU activation, Dropout, and then the second convolutional layer. The second convolutional layer is followed by 1D BatchNorm, a GELU activation, and its output is added to the other path. The sum of the two paths then goes through a GELU activation and Dropout.

Additional parameters Throughout each of the models we use a 0.1 dropout for both pre-training, and fine-tuning. Moreover, during the fine-tuning stage, when the pre-train head is replaced with the linear classification layer, we add a 0.5 Dropout layer before the linear classification layer. This is to reduce overfitting on the (often small) fine-tuning datasets.

Middle and high data regime results

Given the large size of the tables that display the result, we decided to only show the lowest data regime (the smallest percentage of training + validation available) in the main paper, see Table 1. In the following two subsections, we show the middle and high regime results for each of the datasets and each of the models. The models are trained the same way as outlined in the main text.

Middle-data regime

Dataset	EMG@50%			ECG@1%			PPG@20%			HAR@20%		
Metric	ACC	ROC	PRC	ACC	ROC	PRC	ACC	ROC	PRC	ACC	ROC	PRC
PatchTST (s)	78.37	89.91	84.03	56.34	52.92	61.79	57.07	73.92	53.98	75.11	91.05	76.52
PatchTST (p)	65.32	80.0	70.9	60.04	53.23	61.86	58.73	73.8	54.56	68.27	88.89	70.99
bioFAME (s)	63.95	78.8	70.97	63.39	52.46	61.21	58.62	74.99	55.85	59.25	86.77	63.77
bioFAME (mp)	78.67	93.8	88.33	69.78	53.35	61.85	57.62	75.01	55.48	65.81	88.73	70.19
NLPatchTST (s)	85.77	95.29	90.9	58.5	52.76	61.35	58.21	74.08	54.43	76.27	91.49	77.89
NLPatchTST (p)	86.89	96.04	92.45	56.99	52.89	61.47	59.22	74.67	55.54	72.13	90.23	74.12
NLPatchTST (mp)	86.01	95.3	91.5	59.01	53.26	61.75	58.43	74.48	55.22	68.28	88.76	70.8
SimMTM (s)	90.21	97.0	93.12	<u>77.76</u>	55.12	63.48	55.26	<u>77.72</u>	<u>58.74</u>	78.85	92.02	81.34
SimMTM (p)	86.05	94.01	90.59	<u>62.82</u>	54.01	62.32	54.76	<u>76.98</u>	<u>58.31</u>	79.24	92.28	81.99
Ci (s)	98.16	99.1	97.77	73.28	55.74	64.24	<u>60.08</u>	75.61	57.11	84.15	93.86	85.6
Ci (p)	96.37	99.26	98.42	70.58	55.27	63.73	58.94	75.86	57.23	78.95	92.72	82.13
CiTrus (s)	<u>98.15</u>	99.58	99.72	<u>73.36</u>	<u>55.95</u>	<u>64.4</u>	59.67	74.15	55.26	79.14	92.19	80.87
CiTrus (p)	<u>97.29</u>	<u>99.4</u>	<u>98.54</u>	71.49	55.61	64.18	58.93	75.7	<u>58.42</u>	<u>82.06</u>	<u>92.87</u>	<u>82.64</u>
CiTrus (fp)	97.05	<u>99.28</u>	<u>98.55</u>	86.76	56.48	64.96	63.9	81.65	65.27	75.13	90.38	76.18
CiTrus (mp)	96.08	98.52	97.09	72.94	<u>55.96</u>	<u>64.66</u>	<u>60.41</u>	75.62	58.2	<u>82.17</u>	<u>92.96</u>	<u>82.79</u>
Dataset	FDB@1%			Epilepsy@5%			Gesture@20%			SleepEDF@1%		
Metric	ACC	ROC	PRC	ACC	ROC	PRC	ACC	ROC	PRC	ACC	ROC	PRC
PatchTST (s)	55.04	55.23	38.86	95.49	97.89	99.28	52.59	86.18	59.74	69.8	68.03	36.41
PatchTST (p)	62.18	56.8	40.29	95.42	97.67	99.12	58.17	88.24	65.88	71.01	68.03	36.08
bioFAME (s)	53.18	54.4	37.97	95.02	97.93	99.38	39.51	81.63	48.31	71.08	69.29	38.74
bioFAME (mp)	58.96	58.04	41.14	95.03	97.97	99.37	45.67	83.9	54.13	71.26	69.19	<u>39.37</u>
NLPatchTST (s)	63.55	58.05	41.15	85.58	81.28	90.22	54.02	86.33	59.9	68.29	67.84	36.26
NLPatchTST (p)	66.04	58.12	41.31	94.64	96.21	98.41	57.86	88.05	66.14	72.81	68.8	38.07
NLPatchTST (mp)	68.04	58.96	41.88	94.97	96.83	98.72	<u>59.38</u>	<u>88.28</u>	<u>67.35</u>	71.16	68.01	36.5
SimMTM (s)	64.03	60.88	44.55	95.45	55.31	87.07	<u>64.46</u>	<u>89.55</u>	<u>71.81</u>			
SimMTM (p)	80.71	66.3	50.64	94.56	55.28	87.27	65.71	90.06	72.07			
Ci (s)	84.27	68.14	54.51	95.56	<u>98.71</u>	<u>99.58</u>	57.01	88.07	63.54	<u>74.43</u>	70.29	40.24
Ci (p)	<u>82.03</u>	<u>67.55</u>	<u>53.42</u>	96.15	98.83	99.63	50.8	86.38	58.81	75.12	<u>69.87</u>	<u>40.12</u>
CiTrus (s)	80.6	67.26	52.9	95.46	<u>98.52</u>	<u>99.51</u>	56.61	88.15	63.86	<u>74.19</u>	<u>69.4</u>	<u>38.41</u>
CiTrus (p)	79.13	65.33	49.96	95.58	96.99	98.61	50.18	86.51	59.77	72.42	69.03	38.37
CiTrus (fp)	<u>82.01</u>	<u>67.61</u>	<u>53.21</u>	<u>95.88</u>	98.44	99.47	58.08	86.67	64.88	55.56	62.35	30.13
CiTrus (mp)	76.37	64.97	49.52	<u>95.76</u>	97.61	98.94	59.2	87.82	66.14	70.46	68.07	36.46

Table 19: A comparison of the different model architectures for the middle-data regime. We use the same evaluation method for each model, for EMG and FD-B we interpolate the data for fine-tuning, and for the other datasets we use our sliding window approach. The letters in brackets refer to how the model is trained; (s) is trained from scratch, (p) means it is pre-trained, (mp) means it uses multi-modal pre-training, and (fp) means it uses frequency pre-training. ACC, ROC, and PRC refer to the accuracy, area under the receiver operating characteristic, and the area under the precision recall curve, respectively. The best result for each metric is shown in bold, the second best result is double-underlined, and the third best result is single-underlined.

High-data regime

Dataset	EMG@80%			ECG@2%			PPG@50%			HAR@50%		
Metric	ACC	ROC	PRC	ACC	ROC	PRC	ACC	ROC	PRC	ACC	ROC	PRC
PatchTST (s)	89.4	97.59	95.18	59.57	53.44	61.97	62.34	74.82	56.08	84.3	93.52	84.22
PatchTST (p)	77.95	90.03	82.66	62.53	53.54	61.93	62.18	75.65	56.9	81.04	92.71	81.84
bioFAME (s)	76.89	90.03	81.42	67.24	52.94	61.49	60.91	76.57	55.91	66.44	88.43	69.51
bioFAME (mp)	84.31	95.36	90.76	74.92	54.07	62.41	62.44	76.11	57.43	81.35	92.81	81.64
NLPatchTST (s)	92.77	98.65	96.8	60.73	53.72	61.85	62.02	76.61	58.02	87.06	94.04	85.88
NLPatchTST (p)	93.29	98.32	96.57	59.7	53.18	61.58	61.37	75.36	56.8	85.77	93.77	85.19
NLPatchTST (mp)	91.21	97.72	95.08	61.14	53.45	61.77	62.6	75.74	57.15	84.59	93.5	84.28
SimMTM (s)	93.05	99.04	97.75	68.11	55.02	63.49	59.59	<u>81.11</u>	<u>64.61</u>	82.12	92.72	83.01
SimMTM (p)	92.45	98.73	97.49	62.29	53.87	62.24	59.26	<u>79.11</u>	<u>61.72</u>	82.01	93.0	83.81
Ci (s)	98.88	<u>99.52</u>	98.98	74.44	<u>56.58</u>	65.43	62.01	<u>79.17</u>	61.34	87.55	94.28	<u>86.96</u>
Ci (p)	<u>98.27</u>	99.43	98.89	75.67	<u>55.97</u>	64.13	<u>63.8</u>	78.05	60.21	86.76	<u>94.34</u>	86.89
CiTrus (s)	97.66	99.69	99.76	<u>75.77</u>	56.18	64.72	<u>62.9</u>	77.67	60.21	89.82	94.51	87.71
CiTrus (p)	97.77	99.43	<u>99.26</u>	75.5	56.17	<u>64.92</u>	61.48	77.5	59.26	<u>89.29</u>	94.25	86.87
CiTrus (fp)	<u>98.64</u>	<u>99.66</u>	<u>99.69</u>	88.79	56.6	<u>65.15</u>	67.16	83.21	65.68	<u>89.74</u>	<u>94.32</u>	<u>87.2</u>
CiTrus (mp)	97.92	99.51	98.99	<u>79.05</u>	56.24	64.78	61.36	76.76	57.98	88.12	94.08	86.4
Dataset	FDB@2%			Epilepsy@10%			Gesture@50%			SleepEDF@2%		
Metric	ACC	ROC	PRC	ACC	ROC	PRC	ACC	ROC	PRC	ACC	ROC	PRC
PatchTST (s)	67.8	60.64	43.76	95.94	98.47	99.5	60.98	89.8	68.77	70.71	68.96	38.42
PatchTST (p)	67.58	59.24	42.26	96.25	98.32	99.36	64.29	91.45	72.91	73.02	69.12	38.56
bioFAME (s)	60.19	58.17	41.42	95.52	98.33	99.5	45.49	86.69	55.82	71.72	69.61	39.7
bioFAME (mp)	65.26	61.77	45.46	95.77	98.43	99.51	52.1	88.16	61.26	70.5	69.02	39.33
NLPatchTST (s)	73.81	63.47	46.63	92.01	93.02	96.46	61.56	89.31	68.34	67.69	67.45	36.42
NLPatchTST (p)	72.29	61.52	44.37	95.91	98.21	99.39	64.46	91.23	72.09	<u>75.52</u>	69.4	38.83
NLPatchTST (mp)	74.66	62.37	45.04	95.6	98.13	99.34	65.18	91.45	73.2	<u>72.47</u>	68.7	37.82
SimMTM (s)	78.66	66.18	50.72	<u>96.69</u>	55.36	87.79	<u>73.08</u>	<u>93.18</u>	80.27			
SimMTM (p)	85.32	67.73	52.95	<u>96.41</u>	55.38	87.98	74.2	93.4	<u>79.76</u>			
Ci (s)	88.7	69.0	55.79	96.11	<u>99.13</u>	99.77	61.47	91.34	<u>70.7</u>	72.5	70.19	<u>40.36</u>
Ci (p)	<u>87.46</u>	<u>68.83</u>	<u>55.5</u>	96.75	99.14	<u>99.74</u>	61.7	90.43	69.77	75.81	<u>70.14</u>	40.6
CiTrus (s)	<u>85.03</u>	<u>68.44</u>	<u>54.79</u>	96.37	<u>99.12</u>	<u>99.75</u>	63.04	90.89	71.21	74.84	<u>69.49</u>	38.65
CiTrus (p)	83.86	67.18	52.71	96.45	98.82	<u>99.58</u>	63.26	91.37	71.09	<u>75.38</u>	<u>69.77</u>	<u>39.89</u>
CiTrus (fp)	<u>87.42</u>	<u>68.56</u>	<u>55.05</u>	96.48	98.95	99.69	<u>67.9</u>	<u>92.44</u>	<u>76.12</u>	64.7	66.43	34.68
CiTrus (mp)	83.52	67.28	52.95	<u>96.51</u>	98.57	99.37	62.95	90.23	70.64	72.82	68.56	38.07

Table 20: A comparison of the different model architectures for the high-data regime. We use the same evaluation method for each model, for EMG and FD-B we interpolate the data for fine-tuning, and for the other datasets we use our sliding window approach. The letters in brackets refer to how the model is trained; (s) is trained from scratch, (p) means it is pre-trained, (mp) means it uses multi-modal pre-training, and (fp) means it uses frequency pre-training. ACC, ROC, and PRC refer to the accuracy, area under the receiver operating characteristic, and the area under the precision recall curve, respectively. The best result for each metric is shown in bold, the second best result is double-underlined, and the third best result is single-underlined.